Understanding Surface Water - Groundwater Interaction, Submarine Groundwater Discharge, and Associated Nutrient Loading in a Small Tropical Island Watershed

Christopher K. Shuler[*,a, b], Henrietta Dulai[a, b], Olkeba T. Leta[c], Joseph Fackrell[b], Eric Welch[b], and Aly I. El-Kadi[a, b]

[*]cshuler@hawaii.edu

[a]Water Resources Research Center, University of Hawaii Manoa, USA
2540 Dole St., Holmes Hall 283, Honolulu HI 96822

[b]Department of Geology and Geophysics, University of Hawaii Manoa
1680 East-West Rd, POST 707, Honolulu, HI 96822

[c]Bureau of Watershed Management and Modeling, St. Johns River Water Management District, 4049 Reid St, Palatka, FL 32177

[*] Corresponding author

Abstract

Submarine groundwater discharge (SGD) is recognized as an important nutrient delivery mechanism in coastal ecosystems. However, water quality management in these settings is typically focused on surface waters, often ignoring SGD and nearshore groundwater-surface water interaction. In this study, we integrate a comprehensive radionuclide tracer based field investigation with watershed modeling to examine groundwater – surface water partitioning and to quantify nutrient loading from fresh SGD and streamflow in a small embayment located in American Samoa. Measurements included streamflow, SGD rate, and environmental tracers, including ^{222}Rn concentrations, nutrient levels, and nitrogen isotope values in groundwater and surface water samples. We then used the Soil and Water Assessment Tool (SWAT) to validate measured baseflow and SGD rates, and also to estimate storm flows, which were not measured in the field. Field results showed SGD was a significant delivery mechanism for coastal nutrient loads, whereas baseflow-nutrient loading from the upper-watershed was minimal during the study period. Seepage run measurements informed a conceptual hydrogeologic model of groundwater, surface water, and coastal water interaction, which we applied in developing the watershed model. The SWAT model simulated flow observations satisfactorily, and indicated baseflow accounts for only 39% of the total annual stream flow with surface runoff and lateral flow (i.e. interflow) making up the rest. By examining water and nutrient exchange between groundwater, surface water, and SGD, this study provides a more complete understanding of the fate and transport of water and nutrients in small-island watersheds where anthropogenic activities potentially threaten the health of coastal ecosystems.

Highlights

- Developed groundwater-surface water conceptual model of a steep tropical watershed
- Assessed submarine groundwater discharge and nutrient loading with Radon-222
- Paired field study with watershed model to expand understanding of hydrologic factors

Keywords

- Submarine Groundwater Discharge (SGD)
- Soil and Water Assessment Tool (SWAT)
- Watershed modeling
- Coastal nutrient loading
- Groundwater-stream water interaction
- American Samoa

1. Introduction

Discharge of anthropogenic nutrients to coastal areas has the potential to significantly impact nearshore water quality and affect reef health (Bahr et al., 2015; Dulai et al., 2016). In recent decades, the effect of submarine groundwater discharge (SGD) on coastal nutrient budgets has become widely recognized (e.g., Johannes and Hearn, 1985; Dulaiova et al., 2006; Rodellas et al., 2015), and SGD has been found to be a particularly significant nutrient delivery mechanism in tropical volcanic island settings (Zektser, 2000; Moosdorf et al., 2015; Dulai et al., 2016). Nonetheless, environmental water quality management typically focuses on surface waters, often ignoring SGD. The U.S. Environmental Protection Agency's Clean Water Act (Section 303(d)) requires states and territories to establish water quality standards and Total Maximum Daily Loads (TMDLs) for nutrients in receiving waters. In many places, including the Territory of American Samoa, such standards apply only to fresh surface and open coastal waters (AS-EPA, 2013a), thereby overlooking potentially important nutrient pathways. Spatial variability in groundwater discharge directly to streams may also affect the validity of TMDL measurements, which are assumed to originate from surface water sources only. Recent studies from streams (e.g., Avery et al., 2018), mangrove environments (e.g., Gleeson et al., 2013) and large tidal estuaries (e.g., Makings et al., 2014) indicate that groundwater has significant impacts on both coastal water quality and nearshore stream water quality, underscoring the importance of considering groundwater-surface water interaction when designing water quality monitoring protocols. However, accurate quantification of groundwater discharge to streams and coastlines is inherently challenging because available methods typically rely on measurements and conceptual models with high uncertainties. This underscores the need to develop an improved understanding of how land-use, groundwater, and surface water interact to deliver nutrients to the coast.

The naturally occurring noble gas radon-222 (^{222}Rn) has become one of the most widely used tracers for determining SGD rates, (e.g., Burnett and Dulaiova, 2003; Charette et al., 2007; Sadat-Noori et al., 2015) and when combined with water quality sampling, this method is widely used for estimating associated coastal nutrient fluxes (e.g., Dulaiova et al., 2010; Gleeson et al., 2013; Wang et al., 2017). Radon has also been applied successfully in stream headwaters, channels, and estuaries for investigating the magnitude and locations of groundwater-surface water interactions in terrestrial settings (e.g., Peterson et al. 2010; Cartwright et al., 2011; Unland et al., 2013; Gleeson et al., 2018). However, very few studies have integrated these approaches and investigated groundwater, surface water, and coastal water interactions on a whole watershed scale (e.g. Corbett et al., 1999), and to our knowledge none have done so in a tropical basaltic-island setting. Groundwater becomes enriched in ^{222}Rn through prolonged contact with aquifer material, and pore-water ^{222}Rn concentrations typically reach an equilibrium between ingrowth and radioactive decay within a couple of weeks. After leaving the aquifer, dissolved ^{222}Rn has a short half-life of 3.8 days, exhibits conservative behavior through the full salinity range, and shows low concentrations in surface and ocean waters, making it an excellent tracer of recently discharged groundwater.

Predictable isotopic fractionation of nitrogen (N) in dissolved nitrate and nitrite ($\delta^{15}N_{N+N}$) has been used extensively for tracing sources of nutrients in groundwater (e.g. Kendall and Aravena, 2000; Cole et al., 2006; Hunt, 2007), stream water (e.g. Lindau, et al., 1989), and coastal surface waters (e.g. Garrison et al., 2007; Wong et al., 2014; Wiegner, 2016; Bishop et al., 2017). Commonly referenced ranges for $\delta^{15}N_{N+N}$ values indicate synthetic fertilizer influenced waters have relatively low $\delta^{15}N_{N+N}$ values (-5 ‰ to +5 ‰), natural soil processes typically produce porewaters with intermediate $\delta^{15}N_{N+N}$ values (+2 ‰ to +6 ‰), and manure and human wastewater leachates generally produce higher $\delta^{15}N_{N+N}$ values, albeit with a wide range (+4 ‰ to+25 ‰) (Kendall and Aravena, 2000; Dailer et al. 2010; 2012; Fenech et al., 2012, Abaya et al. 2018a,b). This method does have a number of limitations, for example wastewater influenced $\delta^{15}N_{N+N}$ values in tropical island settings have been found to encompass a wide range, from 5 ‰ to 23 ‰ (Bishop et al., 2017; Amato et al., 2016; Hunt and Rosa, 2009; Rogers et al., 2012). Nonetheless, $\delta^{15}N_{N+N}$ remains a valuable tool for providing clues about nutrient sources, which has made it a widely used source dependent tracer despite well-known limitations (Xue et al., 2009).

In the hydrologic sciences it is common, and some may argue, a standard practice, to integrate numerical models with field-based studies to constrain or validate estimates produced by either method (e.g. Anderson, 1987; Biondi, 2012). The wide spatial coverage of models also makes them useful for management agencies tasked with covering large areas that are difficult to fully characterize with field methods. However, model accuracy depends on appropriate conceptualization of the hydrologic system, and sufficient calibration and validation data to constrain uncertainty and ensure accuracy. Watershed scale, SGD-focused field studies that integrate modeling components (e.g. Michael, 2005; Nakada et al., 2001) often apply groundwater models capable of simulating variable-density flow, such as SEAWAT (Guo and Langevin, 2003) or FEFLOW (WASY, 2004). However, calibration data for these fairly complex models is often limited, leading to overparameterization, and problems with equifinality (Kirchner, 2006). On the other hand, availability of above-surface hydrologic data is typically better due to the existence of nation-wide meteorological and streamflow measurement networks (Slack and Landwehr, 1992; NRC, 2004). These data can be used to calibrate watershed models such as the Soil & Water Assessment Tool (SWAT) (Arnold et al., 1998; Gassman et al., 2007, 2014) or Gridded Surface/Subsurface Hydrologic Analysis (GSSHA) (Downer and Ogden, 2006) that apply the water budget approach to partition hydrologic inputs between different pathways. By using a water budget approach, watershed models are also able to produce estimates of subsurface inputs and returns to surface waters without requiring difficult to obtain subsurface data. Although watershed models lack the fine scale resolution available with groundwater models, at the watershed scale, these models can provide some of the same benefits where more detailed subsurface simulation is not needed. (e.g. Oberdorfer, 2003; Lee and Kim, 2007).

In American Samoa, anthropogenic nutrient loading and sedimentation to coastal zones have been identified as primary factors in reducing the reef's ability for recovery from increasing environmental stressors (McCook, 1999; Craig, 2009). Long-term studies of reefs on Tutuila, the territory's main island, suggest SGD is likely to be a significant explanatory variable in reef health (Houk et al., 2013; Whitall and Holst, 2015). However, prior to this study, there have been no known attempts to quantify SGD and its associated nutrient loading in American Samoa. To fill this gap, we used measurements of environmental tracers including ^{222}Rn, dissolved nutrients, and nitrogen isotopes to trace groundwater discharge, partition baseflow and fresh SGD nutrient flux, and explore probable nutrient sources within a small, tropical-island watershed and embayment. Field observations provided insights for informing conceptual model development and were useful for model calibration and validation. Watersheds in American Samoa provide unique settings to examine nutrient budgets on a basin-wide scale due to small drainage areas, relatively good accessibility, and high precipitation rates that drive measurably significant water fluxes.

In this study, we hypothesize that multiple hydrologic pathways, including groundwater, surface water, and fresh SGD all act as significant controls on coastal nutrient loading in small tropical watersheds, exemplified by those of American Samoa. To investigate this question, we integrated a detailed geochemical field investigation with watershed modeling in order to partition the impact of water and nutrient discharge from different hydrologic pathways. Our primary objectives are to develop a better understanding of groundwater, surface water, and coastal water interaction, and to quantify coastal nutrient loading impacts from non-point sources in tropical island watersheds.

2. Study Area

Faga'alu Watershed consists of a small (2.1 km^2), steep, heavily forested valley with one main perennial stream draining into Faga'alu Bay, a small arm of Pago Pago Harbor (Fig. 1). Geologically, the watershed is carved from dense inner-caldera basalts formed about 1.2 mya, and the valley bottom is filled with a gently inclined wedge of terrestrial and marine alluvium that extends about 1 km upstream from the coast (Stearns, 1944). The regional scale aquifer permeability of the inter-caldera basalts is likely to be significantly lower than that of the terrestrial alluvium, based on aquifer properties of similar geologic units in Western Tutuila (Izuka et al., 2007). However, in Faga'alu the only known well is located in the alluvium, precluding direct comparison of each unit's hydrogeologic properties. Significant springs found in the inter-caldera unit indicate that it contains high-level groundwater, which is likely to be impounded by sub-surface structures, such as dikes, perching layers, or potentially faults

(Davis, 1963). In the upper watershed, the soil type is primarily silty clay to clay loam Lithic Hapludolls ranging from 20–150 cm deep, and the alluvial unit is covered with a fairly deep (>150 cm) mixture of well-drained very stony silty clay loams and poorly-drained silty clay to fine sandy loams (Nakamura, 1984). Faga'alu's climate is warm and humid with year round average temperatures around 28°C and annual rainfall between 3000 and 6000 mm/year, depending on elevation. The wet season extends from October to May and the drier season spans June to September.

In Faga'alu, anthropogenic activities have been connected to recent degradation of reef health and reduction of stream water quality, leading to its designation as a federal priority watershed management area by the United States Coral Reef Task Force (Sauafea-Le'au, 2013). Both stream and coastal water quality in Faga'alu have been classified as 'impaired' since 2006 (AS-EPA, 2016) and American Samoa Environmental Protection Agency (AS-EPA) coral reef monitoring suggests that Faga'alu's benthic ecosystem is one of the most impacted on the island (Houk et al., 2005). Previous studies implicate the stream as a pathway for terrigenous sediments and excessive nutrient loads to the bay (DiDonato, 2005; Messina, 2016; Messina & Biggs, 2016). However, the role of groundwater as a hydrologic pathway for terrigenous contamination remains unconstrained. The three primary anthropogenic nutrient sources on Tutuila have been previously determined to be: (1) On-Site wastewater Disposal Systems (OSDS), (2) widespread small-scale pig farming operations, and (3) agricultural fertilizers (Falkland et al., 2002; Polidoro et al., 2017; Shuler et al., 2017); but the relative impact of each source on coastal ecosystems remains poorly understood.

3. Methods

3.1 Water Sampling and Stream Gauging Methods

We collected groundwater, coastal water, and stream water samples throughout a weeklong sampling campaign in the dry season of 2014 during a period with no significant rainfall. This included a longitudinal sampling and measurement transect up Faga'alu stream, hereafter referred to as a seepage run (Rosenberry and LaBaugh, 2008), which we conducted during a single 24-hour period through the lower 1 km stream section. During the seepage run, we measured streamflow at ten separate locations with a Price-type Pygmy Current Meter and the velocity-area-method (Turnipseed and Sauer, 2010) and sampled stream water at seven of those locations throughout the reach between Faga'alu Quarry, and the lowest section of stream that was not affected by the tide during the sampling period. During a boat-based coastal water survey (see section 3.2.2), we collected coastal water samples from Faga'alu Bay one day after the seepage run. We identified three areas along the shoreline of the bay with brackish coastal springs, and sampled these twice each at low tide throughout the week. We also sampled the only production well in the valley (Well #179). All sampling locations are shown on Fig. 1, and streamflow data are given in supplementary material Tables A1 and A2. To verify the seepage run results, we conducted a second seepage run on August 10th, 2016, and measured streamflow and dissolved ^{222}Rn concentrations (but not nutrients or other parameters) at many of the same sites as in 2014. To reduce measurement uncertainty, streamflow for the second seepage run was measured with a SonTek FlowTracker Handheld Acoustic Doppler Velocimeter, which has a higher velocity resolution and accuracy than the Pygmy meter we used in 2014. Sampling and analysis for ^{222}Rn concentrations was performed in the same way as was done in 2014. With all direct streamflow measurement values, we conservatively assumed a measurement error of 10%, as typical standard errors with pygmy meters have been reported to be between 3% and 6% (Sauer and Meyer, 1992), and field-calculated measurement uncertainties for FlowTracker data were always well below 10%. For all nutrient samples, we also collected in situ temperature, salinity, pH, and dissolved oxygen data with a YSI multiparameter sonde (6600V2-4 model). Nutrient and isotope samples were collected in acid washed 60 ml HDPE bottles triple-rinsed with sample water before filling. Nutrient samples were kept refrigerated, whereas N-isotope samples were frozen until analysis. All nutrient and isotope samples were filtered through 0.45 µm capsule filters, thus all measured nutrient concentrations and comparable modeled nitrogen concentrations reported here refer to dissolved species unless the particulate fraction is specifically indicated. We collected grab samples for ^{222}Rn in 250-ml glass bottles with no headspace and analyzed them the same day as collection with a RAD H_2O radon in water analyzer, manufactured by Durridge Inc. (Billerica MA, USA). Because of ^{222}Rn's short half-life (3.8 days), ^{222}Rn grab sample values were decay corrected to the time of collection.

We analyzed all water samples for dissolved nutrients including nitrate and nitrite (N+N), ammonium (NH_4^+), phosphate (PO_4^{3-}), silicate (Si), total dissolved nitrogen (TDN), total dissolved phosphorus (TDP), dissolved ^{222}Rn concentration, and nitrogen isotope ($\delta^{15}N_{(N+N)}$) values of N+N in samples having > 1 µmol/L of N+N. The only exceptions were samples collected in 2016, which were only analyzed for ^{222}Rn concentrations. Nutrient samples were analyzed within two weeks of collection at the University of Hawaii School of Ocean and Earth Science and Technology (SOEST) Laboratory for Analytical Biogeochemistry using the methods described in Armstrong et al. (1967) and Grasshoff et al. (1999). Nitrogen isotope samples were measured within 4 months of collection at the University of Hawaii's Stable

Isotope Biogeochemistry Lab using the denitrifier method of Sigman et al. (2001). Isotopic results are expressed here in per mil (‰) notation relative to the isotopic reference standard of AIR.

Coastal groundwater is composed of both oceanic and fresh water. However, because this study focuses on assessing nutrient flux from terrigenous sources only, the oceanic component in coastal spring samples was mathematically unmixed to reveal nutrient levels of only the fresh component of each sample, regardless of seawater dilution. This is commonly done in settings where the subterranean estuary and recirculating seawater are not a significant source of nutrients (Street et al., 2008), and was performed here with an unmixing calculation (e.g., Hunt and Rosa, 2009) that assumed conservative nutrient behavior during mixing and was based on an oceanic end member from Tutuila. This calculation allowed the derivation of nutrient fluxes solely contributed by fresh groundwater. We collected duplicate samples at five locations and analytical uncertainty was assessed using the relative percent difference (RPD) method, which is defined as the absolute value of the difference between two duplicates, expressed as a percentage of their mean. Average RPD was 1.4% for N+N, 0.5% for Si, 0.6% for PO_4^{3-}, 2.4% for NH_4^+, 0.8% for TDN, 1.9% for TDP, and 6.8% for $\delta^{15}N_{(N+N)}$. In about half of the samples, concentrations of PO_4^{3-} were measured to be slightly greater than TDP. This is likely due to small inconsistencies between the two analysis methods, and suggests that in most of the samples collected, nearly all of the TDP is in the form of orthophosphate.

3.2 Radon-Based SGD Field Estimates

Dissolved ^{222}Rn was used as a groundwater tracer in a temporally and spatially distributed non-steady-state radon flux model to calculate bay-wide SGD rates following the methods of Burnett & Dulaiova (2003) and Dulaiova et al. (2010). We assessed temporal (tide-dependent) variability with a time-series of ^{222}Rn measurements taken from a fixed nearshore location over a 48-hour period. This was coupled with a coastal water survey to assess spatial variation in ^{222}Rn throughout the inner bay. For both the time-series and survey, ^{222}Rn concentrations were measured by pumping surface water through an air-water exchanger connected to a radon-in-air monitor (RAD AQUA, Durridge Inc.). To obtain bay-wide SGD fluxes, we scaled up the tidally-averaged SGD flux from the stationary time-series to account for the additional SGD flux observed during the coastal survey in locations adjacent to the time-series location, as described below.

3.2.1 Stationary ^{222}Rn Time-Series

The ^{222}Rn time-series instrument package used a peristaltic pump that pumped surface water from the bay to an instream flow cell (with no headspace) attached to the YSI 6600-series sonde that continuously logged water salinity and temperature. The inlet hose for the pump was connected to a moored float located at a stationary point in the bay about 50 m away from the stream mouth (Fig. 1). After passing through the YSI, water flowed into an air-water-exchanger where ^{222}Rn gas was extracted and pumped to the RAD7. Tidal height was measured by a pressure transducer placed on the seafloor at the float anchor. We deployed the instrumentation for about 48 hours and the RAD7 was set to integrate measurements of ^{222}Rn activity every 30 minutes. Typically, SGD manifests as a fresh or brackish plume that overlies denser seawater. We measured plume thickness at low tide by manually conducting salinity depth profiles at the water intake, and this plume thickness was used for volumetric calculations in the ^{222}Rn mass-balance model. Change in plume thickness due to tidal dilution was calculated by subtracting the thickness of the underlying salt-water layer from the total depth of the water column.

3.2.2 Coastal Water Survey

We performed the coastal water survey once the time-series was finished, during a 3-hour period bracketing low tide. We transferred the time-series instrument platform to a small boat and rowed throughout the bay while the air-water exchanger was supplied with surface water from a bilge pump tethered to the hull of the boat. The RAD7 was set to integrate ^{222}Rn activity every 5 minutes and data was resampled to one minute intervals yielding a total of 205 points available for interpolation. During the survey, three distinct plumes of SGD were detected as low salinity and high ^{222}Rn anomalies. We refer to these plumes as the southern, central, and northern plumes. During analysis, the surface area and geometry of each plume was determined by nearest neighbor interpolation of measurement points and contouring of the resultant ^{222}Rn activity surface. Boundaries for each of the three plumes were defined as the ^{222}Rn-isoline representing the mid-point of the range of measured activities (3.25 dpm/L). We defined the bottom boundary of each plume to be the salinity 28 isohaline, as indicated by salinity depth profiles that we took periodically during the survey; or if salinity was consistent throughout the whole water column, the full water depth was used as the plume thickness. Note that the time-series measurement described in section 3.2.1 was performed at a location that fell inside of the central plume. Additionally, during the survey, coastal water samples were collected for analysis in the same manner as stream and groundwater samples.

3.2.3 SGD Flux Scaling, Fresh and Recirculated Fractions

The ^{222}Rn flux model modified from Dulaiova et al. (2010) was used to calculate SGD fluxes for both survey and time-series data. The model uses a mass-balance approach that relies on accounting for ^{222}Rn losses and additions from local and offshore processes that are not related to SGD. We assumed that ambient ^{222}Rn activities from oceanic or atmospheric sources were comparable to those found in the Hawaiian Islands, and used an ambient ^{222}Rn activity of 0.03 dpm/L (Kelly and Glenn, 2012), a local excess ^{222}Rn activity of 0.08 dpm/L supported by in situ ^{226}Ra (Street et al., 2008), and an offshore ^{222}Rn activity of 0.087 dpm/L, derived from the offshore ^{226}Ra (Fröllje et al., 2016). We assumed residence time of SGD affected-groundwater within Faga'alu's inner bay to be 12.2 hours, the length of one tidal cycle, which is within the ranges of published residence times from water circulation studies of Faga'alu (Storlazzi et al., 2014; Vetter and Vargas-Angel, 2014). Hourly measurements of local wind speed and air temperature were obtained from the American Samoa Observatory NOAA Earth System Research Laboratory (ESRL) weather station at Cape Matatula. To assess the SGD endmember composition, we collected groundwater samples from the only well in the valley and from four coastal spring locations at low tide. The ^{222}Rn activity measured in coastal springs and the well showed a linear mixing relationship with salinity (Fig. A1, supplementary material), which suggests that while seawater recirculation does occur, the nearshore reef substrate or the re-infiltrated coastal water does not add a significant quantity of ^{222}Rn to groundwater during this process; likely because circulation is rapid and recirculated seawater does not spend enough time in the subsurface to collect measurable radon. The linearity of this relationship also indicates the fresh coastal spring ^{222}Rn endmembers (when corrected for dilution by seawater) are quite consistent with the ^{222}Rn activity measured at Well

179. Therefore, the ^{222}Rn concentration from the well was used as the groundwater end member for fresh SGD calculations, and the standard deviation of all measured salinity-unmixed ^{222}Rn concentrations (Table 1), which equaled ± 54 dpm/L or about 44% of the ^{222}Rn endmember value was used as the uncertainty on this quantity, to be propagated through SGD calculations. It should be noted that by using the fresh groundwater ^{222}Rn endmember for SGD calculations, only the fresh SGD rate was calculated, assuming that the recirculated fraction did not carry a ^{222}Rn signature. This assumption was indicated by high-salinity, low-^{222}Rn water found at coastal springs most likely resulting from seawater intrusion to the coastal aquifer at high tide on relatively short time scales. Further this assumption is discussed in section 5.4.1. Please note that all future references to SGD in this work indicate fresh groundwater discharge only.

The time-series calculations provided a temporally-integrated SGD rate, but for the central plume only, as this was where the water intake was located. On the other hand, the coastal water survey provided spatially distributed SGD rates, which allowed for the identification of three distinctive SGD plumes, but only as a snapshot in time. Therefore, to calculate temporally integrated SGD flux to the whole bay, the ratios of survey-based SGD rates in the northern and southern plumes to the survey-based SGD rate in the central plume were used as scaling factors to upscale the time-series derived, temporally-averaged SGD flux to include the other two plumes. Limitations of this approach included needing to make the simplifying assumptions that tidal variation in the central plume was representative of the other two plumes, that SGD only discharges from the three identified plumes, and that the relative magnitudes of discharge from each plume stay consistent over time. These limitations could be addressed by replicating the survey at different times or repeating the time-series in different locations. However, due to the significant amount of time required for just one time-series and survey, we were unable to conduct the approach repeatedly.

3.3 Watershed and Land-Use Modeling

We used SWAT, a physically-based, semi-distributed, watershed scale, ecohydrological model (Arnold et al., 1998) to calculate transient estimates of flow through different hydrologic pathways (i.e. water budget components). These pathways included surface runoff, lateral flow (i.e., subsurface stormflow), baseflow, and groundwater recharge at different spatial and temporal scales. We also applied SWAT's N-transport capabilities; however, limitations in the availability and quality of existing nutrient data prevented satisfactory calibration of this portion of the model. The wide applicability of SWAT under various conditions and to different environmental problems has been demonstrated worldwide (e.g. Gassman et al., 2007 and 2014; Dadhich and Nadaoka, 2012). The SWAT model was set up with the following input data (Fig. 2):

- A 3x3 m Digital Elevation Model (DEM) from the National Geophysical Data Center ([dataset] NGDC, 2013) and obtained from NOAA Ocean and Coastal Services Center.
- 1:24,000 scale soil maps from the Natural Resources Conservation Service - Soil Survey Geographic (SSURGO) database.
- A 2.4 x 2.4 m 2010 land-use map from the Coastal Change Analysis Program (C-CAP).

The hydrologic portion of the model was parameterized using daily rainfall and streamflow data, which were collected for a different study, but provided to us for this work by A.M. Messina (2016 personal communication, with supporting methodology documented in

Messina, (2016)). These data were collected at two sites within Faga'alu Watershed during the period 2012 to 2014. Daily wind speed, relative humidity, and maximum and minimum temperatures were only available at one of these sites. Solar radiation was measured at the nearby American Samoa Community College ([Dataset] ASCC, 2018) and additional relative humidity data were obtained from the NOAA- Earth System Research Laboratory weather station. The watershed was divided into 26 sub-basins and 403 hydrological response units (HRUs), with zero threshold values for land-use, soil, and slope classes. The model simulation was run for the period of 2005 to 2014.

Available data constraining the locations and magnitudes of anthropogenic nutrient sources in Faga'alu Watershed were collected for SWAT's nutrient loading module. Locations of seventy-four OSDS units, six piggeries, and 1.15 acres of agricultural lands were identified, and are shown in Figure A4 in the supplementary material. Although we parameterized, sensitivity tested, and worked diligently to calibrate SWAT's nitrogen budget module with the goal of predicting N-loads in different hydrologic pathways, we were not able to satisfactorily calibrate the nutrient loading module above acceptable thresholds as defined in section 3.3.1. This was likely due to large uncertainties in calibration data and unreasonably large error-bounds on results, even with the best-fitting model run. Still, the nutrient loading portion of the model was useful for exposing where data gaps exist. Methods used for the nutrient loading model set up are documented in supplementary material in section S2.

3.3.1 SWAT Model Hydrologic Calibration

For managing the calibration process, we used the SWAT Calibration and Uncertainty Program (SWAT-CUP) (Abbaspour, 2014) with the sequential uncertainty fitting (SUFI-2) method of Abbaspour, et al. (2007). Prior to calibration, we ran a sensitivity analysis using the global Latin Hypercube-One-factor-At-a-Time (LH-OAT) method (Van Griensven et al., 2006) as implemented in SWAT-CUP, in order to identify which parameters to use for model calibration. The top three parameters to which the model was most sensitive for flow were: (1) the runoff curve number at soil moisture condition II, (2) the effective stream channel hydraulic conductivity, and (3) the threshold depth of water in the shallow aquifer required for return flow to occur. Lists of all calibration parameters used for flow and nutrient calibration are provided in supplementary material Tables A3 and A4, respectively, and are ordered by the most to least sensitive parameter.

We calibrated the hydrologic portion of model using daily streamflow observations (Messina, 2016) for the period 2012 to 2014 from two sites on lower Faga'alu Stream. The deep-aquifer partitioning coefficient (RCHRG_DP) was adjusted to match field-estimated SGD as well as possible, which allowed measured and modeled baseflow rates to be compared for validation (see section 4.5). The first seven years of the model simulation period (2005-2011) were assigned as model warm up, while the period from 2012 to 2013 was used for calibration. We used the year 2014 as a validation period. We evaluated SWAT performance by using the Nash-Sutcliffe Efficiency (NSE) metric (Nash and Sutcliffe, 1970) and assessed the proportion of observations that were bracketed at 95% model prediction uncertainty (95PPU) interval. We ran SUFI-2 for 1000 simulations, but the 95PPU was estimated only for those simulations (parameter sets) that provided a behavioral solution with NSE threshold value of ≥ 0.5. The temporal evolution of observed daily streamflow hydrographs was reproduced by SWAT with NSE values ranging between 0.65 to 0.86 for both calibration and validation periods, indicating the ability of the model to simulate daily stream flow reasonably well (Fig. 3). The streamflow simulation uncertainty was assessed by examining the number of observations bracketed at the 95% PPU for both the calibration and validation periods, which ranged between 57% to 87% of the observations. For most gauging sites and years, the calculated 95PPU values were above the generally accepted value of (≥ 70%), as recommended by Abbaspour et al. (2015), except for the lower gauging station that had only 57% of the observations bracketed but only during the 2014 simulation period.

3.3.2 SWAT Model Nutrient Transport Calibration

We based calibration for the nutrient flux portion of the SWAT model on a set of twenty NO_3^- and NH_4^+ nutrient measurements also taken between March 2013 and February 2014 by A. M. Messina (2018, personal communication). These measurements represented the only known long-term dissolved nutrient dataset available for this location and time period. The samples were analyzed as described in McCormick (2017) and measurement uncertainty was assessed by concurrently analyzing independent standards with known concentrations. Measurement error reported by McCormick ranged from 7% up to 30%, which limited confidence in these data. The nutrient transport calibration used the same methods as the hydrologic portion of SWAT, with the top three most sensitive nutrient parameters being: (1) the filtration capacity of stream edge, (2) the denitrification threshold soil water content, and (3) the in-stream rate constant for hydrolysis of organic N to NH_4^+.

Unfortunately, it was not possible to calibrate the model to the point where ≥ 70% of the observations were bracketed at the 95% PPU. Model calibration attempts were suspended with the best simulation only able to bracket 60% of the calibration data (nine of the NH_4^+ measurements and fifteen of the NO_3^- measurements) at the 95% PPU. To achieve even this level of calibration, the parameter space had to be expanded to such a large width that the utility of the results was significantly limited.

4. Results

4.1 Conceptual Hydrogeologic Model

By integrating information about the study area's underlying geology with geochemical and physical measurements, we were able to develop a simple conceptual model of Faga'alu's groundwater, surface water, and coastal water interaction during baseflow conditions (Fig. 4). In its upper reaches, dense trachyte and older lava flows underlie the stream (Stearns, 1944), and dikes may also serve to impound groundwater in the shallow subsurface (Davis, 1963). On basaltic islands, dikes or low-permeability structures commonly impound groundwater at high-elevations (Takasaki and Mink, 1985). On a hike to the upper portion of the watershed, we observed numerous springs and small tributaries, indicating a general net transfer of groundwater to surface water in this area. Davis (1963) also documents the significance of springs in the upper Faga'alu watershed based on their historical water usage. Although this spring water is expected to be enriched in ^{222}Rn upon discharge, numerous waterfalls and high turbulence throughout the upper-reaches promote evasion, which significantly reduces ^{222}Rn concentrations as the water flows downhill. At Faga'alu Quarry, which lies at the upper edge of Faga'alu Village, the stream channel slope declines, and the lithology changes to an alluvial valley-fill, likely with higher permeability (Izuka et al., 2007). In the portion of the stream underlain by alluvial-fill, we observed low ^{222}Rn levels and declining streamflow (except where two very small tributaries between sites S5 and S6 were seen to contribute water to the main branch), suggesting the stream is probably losing water to the aquifer in this reach (see section 4.2 below). Once the stream nears the coast, streamflow, ^{222}Rn, and nutrient values spike, indicating this is an area of groundwater discharge, likely from a basal-lens aquifer within the alluvium. When corrected for mixing with high-level baseflow, the nutrient signature of this basal-lens baseflow is a fairly close match to the composition of salinity unmixed coastal spring discharge, suggesting that both of these water sources originate from the same nearshore aquifer.

At the shoreline, coastal springs were found to have variable salinities, indicating the presence of recirculated SGD. However, we also found that concentrations of ^{222}Rn in spring waters varied linearly with salinity (Fig. A1 supplementary material), suggesting that recirculated seawater, at least at shallow depths, does not spend sufficient time in the subsurface for significant ^{222}Rn ingrowth to occur. Previous studies in coastal aquifers show it is possible for fresh SGD to manifest as a separate layer above a deeper saline SGD fraction (Robinson et al. 2007; Kuan et al. 2012). If this were the case in Faga'alu, longer-residence time recirculated SGD might be discharging at depths below detection of our survey methods. Although we did not detect any ^{222}Rn which we can attribute to a deep saline SGD source, such a situation would not be surprising considering the abrupt bathymetry in Faga'alu Bay. In the inner portion of the bay, the substrate is primarily composed of a shallow fringing reef sitting in 1-2 m of water, but with very steep slopes at its margins where depths rapidly plunge to around 25 m. Fringing reef wedges in American Samoa have been hypothesized to have lower hydraulic conductivities than underlying basaltic rocks (Houben et al., 2018), which might contribute to the confinement of deeper SGD until reaching the reef margin, where it could discharge at depth. Future deep-water surveys along the reef margin would be useful for exploring this hypothesis further.

4.2 Characterization of Baseflow Components

Dissolved ^{222}Rn concentrations in the stream were generally low (6-10 dpm/L), except at the two sites nearest the coast (sites S1 and S2), where values increased up to 42 dpm/L. Coincident with increased ^{222}Rn concentrations between the uppermost (S10) and lowermost (S1) sites, were increases in flow from 2,700 to 3,524 m^3/d, DIN concentrations from 4 to 12 µmol/L, and $\delta^{15}N_{(N+N)}$ values from 4.5 to 11.5‰ (Fig. 5). The simultaneous increase in $\delta^{15}N_{(N+N)}$ and DIN input suggests a portion of this DIN may be derived from human or animal waste, which both produce nitrogen with an elevated $\delta^{15}N$ signature (Kendall, 2012). Because there were no observed surface tributaries above the lowest stream sampling sites, the coincident increases in water, nutrients, and ^{222}Rn indicates the stream receives significant basal groundwater discharge just before exiting to the bay. The 2016 seepage run showed almost the exact same pattern, although ^{222}Rn concentrations through the whole stream and particularly near the stream mouth were observed to be higher (up to 122 dpm/L).

Based on these observations, baseflow discharge to the bay can be viewed as a mixture of two distinct components, (1) baseflow sourced from high-level groundwater (Davis, 1963) (here referred to as high-level baseflow) and (2) baseflow sourced from basal-lens groundwater (here referred to as basal-lens baseflow). We estimated the fraction of high-level baseflow (f_S) to basal-lens baseflow (f_{GW}) discharged in the stream estuary with a simple two endmember mixing model applied to ^{222}Rn concentrations using the groundwater end member and surface water from the upper portion of the stream (as measured at site S3):

$$f_{GW} + f_S = 1 \quad (1)$$

$$f_S = \frac{C_{mix} - C_{GW}}{C_S - C_{GW}} \quad (2)$$

Where (C_S) is the average concentration of ^{222}Rn measured at site S3, (C_{GW}) is the ^{222}Rn concentration in groundwater at production well #179, and (C_{mix}) is the mixed sample ^{222}Rn concentration measured at the most coastal stream site, S1. Results from 2014 data indicate stream water at site S1 was composed of 67% high-level baseflow (2,368 m^3/d) and 33% (1,156 m^3/d) recently discharged basal-lens baseflow, and ^{222}Rn-based unmixing results from 2016 data show that stream water at site S1 was composed of 66% high-level baseflow (2,412 m^3/d) and 34% (1,217 m^3/d) recently discharged basal-lens baseflow. Although this calculation relies on some assumptions such as conservative radon behavior (no radioactive decay and no atmospheric evasion over the timescale of the water flow), the partitioning estimate compares very well to the flow increase as directly measured by stream gauging, which in 2014 showed an addition of 957 m^3/d, or an additional 27% between site S3 and site S1 (Table 1) and in 2016 showed an additional flow increase of 37% or an additional 1,339 m^3/d between the lowest site (site S1) and flow at site S3. (Table A2 Supplementary material). When these four separate and independent assessments of streamflow partitioning are averaged, the arithmetic mean fractions of high-level baseflow and recently discharged basal-lens baseflow at site S1 are 67% and 33%, respectively, which were the fractions we used for calculations of nutrient fluxes through these pathways. It should be noted that we did not take nutrient measurements or calculate SGD fluxes in 2016, therefore the 2016 seepage run data was used for streamflow partitioning only.

We calculated baseflow nutrient flux rates by multiplying the respective measured flow rates by the nutrient concentrations observed in each baseflow component (high-level and basal-lens baseflow). Total baseflow loading of DIN and PO_4^{3-} to the bay were estimated to be 0.72 ± 0.08 and 0.38 ± 0.04 kg/d, respectively. When partitioned with equations (1) and (2), basal-lens baseflow was estimated to have delivered 0.47 ± 0.06 kg-DIN/d and 0.16 ± 0.02 kg-PO_4^{3-} /d, whereas only 0.25 ± 0.03 kg- DIN/d and 0.22 ± 0.03 kg- PO_4^{3-}/d were delivered by high-level baseflow (Table 2). Nutrient flux uncertainties were propagated from uncertainties in baseflow discharge and analytical errors of nutrient concentration values.

4.3 SGD Rates and Nutrient Fluxes

4.3.1 Time-Series SGD Fluxes

During the stationary time-series, ^{222}Rn concentrations at the intake point averaged 4.8 dpm/L (range of 2.9 to 8.2 dpm/L), salinities averaged 26.9 (range of 22.3 to 33.1), and the thickness of the SGD-affected brackish plume averaged 38 cm (range of 7 to 70 cm). While the highest ^{222}Rn concentrations and the lowest salinities generally occurred at low-tide, as expected, a continuous input of higher ^{222}Rn and lower salinity water from the nearby stream mouth was also detectable in the time-series data. Conversion of ^{222}Rn concentrations to SGD fluxes with the transient radon balance model yielded an average fresh SGD estimate of 2,959 ± 1,629 m^3/d to the central plume where the intake was located (Fig. A2, supplementary material). However, because the time-series measurement was taken just outside of the stream mouth, the time series and survey points near this area were actually detecting a mixture of

^{222}Rn from coastal SGD and recently discharged basal-lens baseflow from the nearshore tidally-affected part of the stream. Subtracting the basal-lens baseflow fraction (1,156 ± 117 m^3/d) as calculated in section 4.2, left an estimated SGD rate of 1,803 ± 1,633 m^3/d as groundwater coming from the coastal part of the central portion of the bay only. This does assume that most or all of the ^{222}Rn from high-level baseflow has evaded by the time it reaches the coast, which if not, would bias the coastal SGD fraction of the total measured SGD to be a slight overestimate.

4.3.2 Spatial Distribution of SGD from Coastal Survey Measurements

The coastal water survey revealed three distinct groundwater discharge zones, or plumes, one each on the northern, central, and southern portions of the coastline (Fig. 6). We found the highest ^{222}Rn concentrations, up to 7.4 dpm/L, and SGD fluxes, averaging 2,623 ± 1,653 m^3/d, in the central plume, which was centered just to the south of the stream outlet. The southern plume had the lowest ^{222}Rn concentrations and SGD fluxes, up to 4.7 dpm/L and averaging 266 ± 138 m^3/d, respectively, with the northern plume having ^{222}Rn concentrations up to 5.0 dpm/L and SGD fluxes averaging 846 ± 78 m^3/d.

4.3.3 Total SGD and Nutrient Flux Scaling with Coastal Survey Data

The time-series measurement provided critical information about temporal variability in SGD rates, but only for discharge to the central plume. Therefore, to calculate tidally-integrated average fresh SGD fluxes to the whole bay, the time-series estimated discharge was upscaled to include discharge from the northern and southern plumes as well, using the spatially distributed SGD information from the survey as described in section 3.2.3. Calculated scaling factors were 0.10 ± 0.08 for the southern plume and 0.32 ± 0.21 for the northern plume, or in other words, SGD rates estimated during the survey showed the southern and northern plumes discharged 10% and 32%, respectively, of the central plume's SGD rate (see section 4.3.2). Bay wide SGD flux was calculated by multiplying these factors by the central plume's tidally averaged and baseflow corrected SGD rate (1,803 ± 1,603 m^3/d) and summing flux from all three plumes, which yielded an estimated SGD rate of 2,587 ± 1,775 m^3/d to the whole inner-bay. We calculated daily nutrient fluxes from SGD by multiplying coastal discharge rates by the average of salinity-unmixed, coastal-spring nutrient concentrations (Table 1). Fluxes were calculated to be 1.38 ± 1.18 kg-DIN/d and 0.40 ± 0.32 kg-PO_4^{3-}/d (Table 2). Nutrient flux uncertainties were propagated from uncertainties in SGD rates and the standard deviation of averaging the nutrient concentration values of coastal spring waters.

Table 1: Measured dissolved nutrient and tracer concentrations in stream (S), well (W), and salinity unmixed samples from coastal springs (Csp)

Sample name	Latitude	Longitude	Salinity (PSU)	DO (mg/L)	^{222}Rn (dpm/L)	N+N** (µM)	PO_4^{3-} (µM)	SiO_4^{4-} (µM)	NH_4^+ (µM)	DIN (µM)	TDN (µM)	TDP (µM)	$\delta^{15}N$ (‰)
S1	14.29131	170.6834	0.2	6.6	42.5	12.5	3.5	522.9	2.00	14.5	19.7	3.4	11.61
S2	14.29153	170.68465	0.1	8.0	15.7	7.2	3.1	518.1	0.10	7.3	11.1	2.9	6.30
S3	14.29147	170.68521	0.1	7.6	6.3	9.1	2.9	530.8	0.27	9.4	14.4	2.9	8.79
S4	14.29082	170.68665	0.1	7.6	6.4	7.9	3.1	530.4	0.24	8.1	12.7	3.4	7.76
S5	14.29053	170.68694	0.1	7.6	6.4	7.9	3.6	519.4	0.41	8.3	12.7	3.4	8.01
S6	14.29008	170.68771	0.1	7.9	10.1	6.2	2.8	499.7	0.21	6.4	9.4	2.6	6.53
S10	14.28877	170.69096	0.1	8.0	-	5.4	2.4	502.8	0.03	5.4	7.8	2.3	4.47
Csp1	14.29046	170.68234	(8.1)*	0.9	62.3	<dl	8.7	299.9	14.08	14.1	17.7	7.9	-
Csp2	14.2896	170.68167	(4.7)*	6.0	101.9	65.9	4.3	522.3	<dl	65.9	60.9	4.1	7.09
Csp3	14.29316	170.68008	(26.7)*	2.5	7.5	39.7	4.1	586.5	1.49	41.2	54.7	3.5	5.50
Csp4	14.29315	170.68008	(26.2)*	0.7	1.2	8.2	7.5	453	21.52	29.7	51.7	6.5	-
W179	14.29092	170.6891	0.2	0.5	124.2	8.3	8.1	632	2.93	11.2	13.6	8.0	5.41
Bay1	14.2918	170.68167	34.8	9.3	6.9	0.5	0.2	3.4	0.58	1.1	5.3	0.4	-
Bay2	14.2929	170.68001	34.7	9.3	3.4	0.7	0.2	7.0	0.63	1.3	5.4	0.4	-
Bay3	14.29234	170.67989	34.9	7.7	1.1	1.0	0.2	1.1	0.41	1.4	5.3	0.4	-
Bay4	14.29041	170.68004	34.6	8.5	0.4	0.6	0.2	7.0	0.47	1.1	6.1	0.5	-
Bay5	14.28957	170.67754	34.9	7.8	0.1	1.0	0.2	3.5	0.41	1.4	5.2	0.5	8.17
Bay6	14.28948	170.67873	34.7	7.9	0.3	1.3	0.3	4.0	0.45	1.8	9.4	0.5	8.56
Bay7	14.29098	170.68172	27.2	7.6	2.7	5.1	1.3	149.4	1.00	6.1	10.2	1.4	-
Bay8	14.29061	170.68221	16.3	7.1	3.1	7.6	2.0	240.1	1.56	9.2	13.8	2.0	8.76
Bay9	14.28965	170.6815	19.4	7.1	4.5	5.9	1.4	161.1	1.06	7.0	11.0	1.4	9.27
Bay10	14.28919	170.68018	31.4	7.0	4.1	1.3	0.3	3.7	0.65	2.0	6.0	0.5	-
Bay11	14.28901	170.67917	34.8	6.2	3.1	1.5	0.3	2.7	0.15	1.7	5.2	0.5	8.62

*Salinities in parentheses are original salinity prior to unmixing from seawater, unmixing was performed to a freshwater salinity of 0.1. Nutrient values in Csp. samples represent fresh endmember values. Note DIN concentrations equal the sum of N+N and NH_4^+.

** N+N refers to nitrate plus nitrate concentration.

4.4 Nearshore Water Quality

In Faga'alu's coastal waters, levels of DIN (1.1 to 9.2 µmol/L) and PO_4^{3-} (0.2 to 2.0 µmol/L) in samples taken near to the shore were higher than those found in samples farther offshore (1.1 to 1.7 µmol -DIN/L) and (0.2 to 0.3 µmol - PO_4^{3-}/L) indicating local terrestrial nutrient sources have a detectable impact on the bay's water quality (Fig. 6). Typically N:P ratios in oceanic waters are near 16:1. However, N:P ratios in Faga'alu's baseflow and SGD are for the most part, disproportionately lower, averaging around 6:1. In Faga'alu's coastal waters, ratios ranged between 7:1 to 20:1 and averaged 12:1 suggesting nitrogen limiting conditions. This shows that SGD not only has an impact on the amount of N and P in the bay but also on the balance of these nutrients, which can have implications for biologic processes that control factors such as eutrophication. Within the bay, nutrient concentrations are elevated in the northern relative to the southern bay (Fig. 6), which is likely caused by circulation within the bay (Storlazzi et al., 2018) as well as heterogeneity in the spatial distribution of SGD. The northern and central plumes show discharge rates that are 5 and 10 times higher than the southern plume, respectively, and the persistent clockwise circulating current (Storlazzi et al., 2014) would be expected to transport stream water and its associated nutrient load to the north rather than to the south.

4.5 SWAT Model Results

Coastally discharging water budget components, otherwise referred to as hydraulic pathways, were simulated directly and indirectly with SWAT. These included baseflow, lateral flow, surface runoff, and SGD, which was interpreted to be equivalent to deep-aquifer recharge, as SGD is not an explicit SWAT model output variable. The SWAT model uses a water budget approach to partition precipitation inputs into evapotranspiration, surface runoff, lateral flow, and groundwater recharge, which is itself partitioned between deep aquifer recharge and baseflow. Using the assumption that the island's groundwater system is in a steady-state, the deep-aquifer recharge calculated by SWAT of 2,578 m^3/d was interpreted to represent fresh SGD flux, as all water recharged to an island's deep aquifer (defined as the region where water no longer interacts with surface water bodies or roots) must eventually discharge as SGD. High-level and basal-lens baseflow were also interpreted from SWAT results by applying our conceptual model, described in section 4.1. The conceptual model shows that stream baseflow originates from two distinctive aquifers, 1) the high-level aquifer and 2) the basal-lens aquifer. To approximate this scenario, we divided the SWAT-calculated baseflow into high-level baseflow and basal-lens baseflow by totaling baseflow from the sub-basins above and below the western margin of the alluvial unit, respectively. Based on this, the SWAT calculated baseflow of 3,203 m^3/d was partitioned into 2,075 m^3/d of high-level, or upper-watershed baseflow and 1,128 m^3/d of basal-lens, or lower watershed baseflow. Comparison between modeled and field measured water balance components showed good agreement, within 2%, 13%, and 0.3% RPD for basal-lens baseflow, high-level baseflow, and SGD, respectively (Table 2). Although streamflow via surface runoff and lateral flow were not measured, the SWAT model provided estimates of these components at 5,888 m^3/d and 2,303 m^3/d, respectively, which sums to about 59% of the total annual stream flow.

Anthropogenic DIN sources used for N input in the SWAT model included piggeries, OSDS units, and agricultural inputs, which together accounted for 2,317 kg-N/yr of N loading to the watershed. The remainder of N inputs to the model were internally calculated in SWAT from natural cycling of organic materials, based on SWAT land-use databases. Limitations in calibration data as well as natural variability of nitrogen distribution potentially due to heterogeneity in sources, pH, and redox conditions, resulted in unacceptably high uncertainties on results of the SWAT nutrient transport module. The level of uncertainty was unsatisfactory for three reasons: (1) less than 70% of the observations, could be bracketed by the 95% PPU, a generally accepted threshold defined by Abbaspour et al. (2015), (2) to achieve a solution where 60% of the calibration data were bracketed by the 95% PPU the range in uncertainty for modeled loading rates encompassed several orders of magnitude, and (3) other model parameters such as rates of N-transformation processes also showed uncertainties ranging across several orders of magnitude, suggesting that these processes were poorly constrained. Simulated ranges in DIN export to the bay (as bracketed by the 95% PPU) through each hydrologic pathway were calculated by the SWAT model to be 0.04 to 2.16 kg-N/d in surface runoff, 0.05 to 1.39 kg-N/d in lateral flow, 0.01 to 0.46 kg-N/d in upper watershed baseflow, 0.12 to 0.59 kg-N/d in lower-watershed baseflow, and 1.74 to 7.41 kg-N/d in deep aquifer recharge (i.e. SGD) fraction. Model calculated rates of N-uptake and denitrification were similarly wide, ranging from 0.38 to 12.9 kg-N/d and 0.69 to 37.8 kg-N/d, respectively, indicating that constraint on these processes was poor. While simulated estimates of DIN export encompassed the equivalent measured fluxes between their upper and lower bounds, this was not surprising considering how large the ranges were. Although the results of the SWAT N-transport simulation were unreliable, this exercise was valuable in that it made clear where current data gaps exist, and underscored the need for a more extensive dataset when calibrating a highly parameterized model such as SWAT. As such, future field efforts should focus on quantifying surface water nutrient concentrations at higher temporal resolutions and across all representative streamflow discharge rates.

Table 2: Comparison of field-estimated flux rates of fresh water and nutrients, and SWAT calculated water fluxes into Faga'alu Bay. Field-based flux estimates are considered snapshot measurements representing the sampling period only, and SWAT calculated values represent the daily average of annual flows through each hydrologic pathway. Note that lateral flow and surface runoff fractions were not measured, but were calculated by SWAT.

Hydrologic pathway	Flow [m^3/d]	DIN load [kg-N/d]	PO_4^{3-} load [kg-P/d]	Flow Modeled with SWAT [m^3/d]	Range in SWAT DIN loads [kg-N/d]
High-level baseflow fraction	2,368 ± 238	0.25 + 0.03	0.22 + 0.03	2,075	0.01 to 0.46
Basal-lens baseflow fraction	1,157 ± 117	0.47 + 0.06	0.16 + 0.02	1,128	0.12 to 0.59
Coastal SGD fraction	2,587 ± 1,775	1.38 + 1.18	0.40 + 0.32	2,578	1.74 to 7.41
Lateral flow fraction	-	-	-	2,303	0.05 to 1.39
Surface runoff fraction	-	-	-	5,888	0.04 to 2.16

5. Discussion

5.1 Implications for Natural Resources Management

Our results indicate SGD is an important factor in coastal nutrient loading in Faga'alu, and likely in other steep basaltic-island watersheds with perennial streams. This is not surprising, as many other studies conducted in similar settings such as Jeju Island and the Hawaiian Islands, have shown SGD may deliver 5 to 62 times the nutrient load of streams (e.g. Garrison et al., 2003; Bishop et al., 2017; Knee et al., 2016, Dulai et al., 2016). Despite these findings, throughout most of the coastal U.S. and specifically in American Samoa, regulatory efforts are primarily concentrated on surface water quality management only (AS-EPA, 2016). Very little regulatory action has been focused on groundwater as a hydrologic pathway for pollution. However, our findings suggest that coastal resource management may be more successful if both groundwater and stream water quality are considered when developing sampling protocols and applying TMDL standards. Although few jurisdictions have even developed groundwater quality standards, (e.g. Kimsey, 2005; N.J.A.C., 2018) American Samoa's small size and strong incentive to maintain fragile reefs could make the territory a reasonable location to pioneer this type of regulatory standard.

Our field results also indicate that impacts to groundwater quality are a major factor on stream water quality. This is an important consideration when designing water quality monitoring protocols. In American Samoa, water quality monitoring site selection is primarily based upon accessibility; some streams are sampled at stream mouths and some are sampled farther upstream (DiDonato, 2004; AS-EPA, 2013b). However, if some stream samples consist of high-level baseflow only, and others taken near the coast contain a fraction of basal-lens baseflow, this reduces the comparability of monitoring results between different streams. This issue could be mitigated by sampling across different stream reaches and considering tidal effects in a standardized manner.

5.2 Conceptual Model Insights

The conceptual hydrogeologic model of groundwater - surface water – coastal water interaction suggested by the results of this study provides new insight into hydrologic processes occurring in small, steep volcanic island watersheds. While geochemical methods similar to those applied here have been used to examine groundwater –surface water interaction in continental streams, estuaries, and wetlands (Genereux et al., 1993; Cook et al., 1998; Gleeson et al., 2013), and also to assess groundwater – coastal water interaction at the shoreline (e.g. Jacob et al., 2009), very few other studies have attempted to trace interactions in water and nutrient flux between hydrologic pathways on a ridge-to-reef scale (e.g. Jarsjö et al., 2007).

The conceptual hydrogeologic model is likely valid in other watersheds around Tutuila and in other high-island settings, specifically where near-shore coastal plains are underlain by more permeable alluvium or marine sediments. Human development is often concentrated in coastal regions, and when sediments underlying developments are more permeable than the surrounding rock, as appears to be the case in Faga'alu, they may facilitate a more direct connection between anthropogenic contaminant sources and basal groundwater. In these areas, groundwater may play a larger role in coastal nutrient transport than surface water. However, the reverse may be true in settings where development is concentrated above less-permeable layers, which has been determined to be the case in Oahu, Hawaii, where a low-permeability marine carbonate formation locally known as "caprock" has been shown to protect the underlying aquifer from contaminants (Oki et al., 1998). Therefore, in basaltic-island settings, the partitioning of nutrients from non-point sources into different hydrologic pathways is likely to be highly dependent on the relative permeabilities of different nearshore geologic layers. This farther underscores the importance of developing an accurate conceptualization of local hydrogeologic systems when designing sampling schemes and assessing nutrient fluxes on a ridge-to-reef scale.

The locality-specific understanding of groundwater-surface water interaction was also useful for interpreting results of the SWAT watershed model. Discharge or loss between groundwater and a stream is generally controlled by water table elevation, which makes this parameter important for predicting the distribution of baseflow in a watershed. However, the

SWAT model uses a simplified linear reservoir model to control loss or gain from groundwater and does not consider water table elevations for baseflow partitioning. This gap is commonly filled by coupling surface water models with groundwater models (e.g. Kim et al., 2008; Guzman et al., 2015). However, subsurface models rely on calibrated parameterization of stream conductance and hydraulic conductivity, and in settings such as Faga'alu, the variable and steep terrain (Kampf and Burges, 2007) as well as a lack of groundwater elevation data (apart from a single well in the valley) imparts large uncertainties to groundwater models. Instead, we used the conceptual hydrogeologic model to determine where the local water table elevation was generally below the stream bed (losing reach below the quarry) and above the stream bed (gaining reach above the quarry, and area proximal to the coast). The model's deep-aquifer – baseflow partitioning coefficient was then adjusted to match field estimated SGD rates. In this manner, measured fluxes from high-level and basal-lens baseflow could be compared against SWAT's estimates, and predictions of surface runoff and lateral flow could be developed, likely within the same or greater certainty as would have been achieved through a more time-consuming and costly groundwater modeling process.

5.3 Nitrogen Source Tracing

While extensive source dependent nutrient tracing efforts were not performed in this study, moderate correlation between elevated DIN concentrations and $\delta^{15}N_{N+N}$ isotopes in baseflow and coastal surface water (r^2 of 0.93 and 0.45, respectively) provided insight into the transport history of nutrients from source to sink. The correlation between $\delta^{15}N_{N+N}$ values and DIN values suggests a large component of sampled DIN originates from a high $\delta^{15}N_{N+N}$ source, such as wastewater or manure, as opposed to synthetic agricultural fertilizers, which typically have $\delta^{15}N_{N+N}$ values near 0 ‰ (Kendall and Aravena, 2000). This result is reasonable, as most agricultural operations in the valley are small and focused on traditional Samoan crops that require few to no chemical inputs. Another management need in American Samoa is to better constrain the impacts of piggeries vs. OSDS-sourced wastewater (Falkland et al., 2002; Shuler et al., 2017). Unfortunately, the overlap of $\delta^{15}N_{N+N}$ values from animal manure and wastewater (Böhlke, 2003), in addition to complications from mixing of nutrients from different sources, prevents the reliable partitioning of DIN from these sources with this method. More specific source-dependent tracers, like microbial source tracing (Scott et al., 2002; Kirs et al., 2011) or wastewater specific compounds (Petrie et al., 2015; Krall et al., 2018) would be useful for separating and prioritizing the impacts between human wastewater and pig manure in Samoa.

5.4 Uncertainties and Limitations

Due to the inherent challenges in measuring SGD, there are many well-known uncertainties associated with using the ^{222}Rn mass balance model approach (Burnett et al., 2007; Schubert et al., 2019). Burnett et al. (2007) describes selection of an appropriate ^{222}Rn endmember activity to be one of the most critical. However, obtaining enough endmember samples to constrain uncertainty is difficult (Knee et al., 2016; Peterson et al., 2008), and Zhu et al. (2019) acknowledges that qualitative judgements are usually a major factor in determining which samples are chosen to represent the endmember. We acknowledge this is the case for this study as well. Therefore, we applied all available information to constrain the SGD ^{222}Rn end-member, including four coastal spring samples (linear salinity unmixing approach yielded a ^{222}Rn endmember value of 116 ± 54 dpm/L), one well sample (measured activity of 124.2 dpm/L), and through rearranging equations (1) and (2), we back-calculated an estimated ^{222}Rn concentration in the basal-lens baseflow of 142.9 dpm/L at stream sample site S1. Although each of these independent observations yielded fairly similar results, additional samples from any of the above would increase confidence in the endmember value used.

Selection of the ^{222}Rn endmember value was also subject to another major assumption; that all of the ^{222}Rn detected was derived from fresh groundwater and not recirculated seawater. We made this assumption because our sampling strategy indicated that of the recirculated SGD detected (in coastal springs), none contained significant levels of ^{222}Rn. This is somewhat surprising as recirculated seawater (with a residence time long enough to pick up a ^{222}Rn signal) is typically a significant part of SGD budgets (e.g. Garrison et al., 2003; Knee et al., 2016). However, as discussed in section 4.1, some studies have suggested it is possible for fresh SGD to manifest as a separate layer above a deeper saline SGD fraction (Robinson et al. 2007; Kuan et al. 2012). If a deeper layer of longer-residence time, saline SGD existed in Faga'alu, we may have missed it by only sampling end-members in the surficial layer. Extreme gradients in the nearshore bathymetry, caused by a potentially low-permeability reef-wedge, can be seen where the reef abruptly plunges from 1-2 m down to 25 m. This feature could have obscured a deep longer-residence time SGD signal from our survey (supplementary material Figure A3). It is feasible that SGD from below the reef wedge may remain unmixed with the shallow waters we sampled. Therefore, even if the coastal spring ^{222}Rn:Salinity ratios found in our samples only represented a surficial layer of fresh SGD, these samples were nonetheless representative of our survey and time-series data. In other words, if deeper, longer-residence time recirculated SGD does occur in Faga'alu then, a) we likely did not detect it, meaning it did not affect our SGD flux calculation, and b) any undetected deep SGD likely did not contain a significant fresh fraction, because this would have caused a discrepancy in the SWAT water budget estimates based on balancing discharge from both baseflow fractions and SGD.

Another uncertainty to consider is the use of assumed ambient ^{222}Rn activities from non-SGD sources. While this is a fairly standard practice (e.g. Burnett and Dulaiova, 2003; Bishop et al., 2016), a reasonable method for assessing the effect of these and other parameters on the final model output is to perform a sensitivity analysis on different parameters of interest. We performed a sensitivity analysis on the ^{222}Rn box-model parameters (Table 3), and the results suggest the ambient ^{222}Rn activity parameters have a negligible effect on the final output.

Table 3: Sensitivity analysis for ^{222}Rn box-model parameters. All parameter values were doubled (multiplied by 2) and halved (multiplied by 0.5) and the resulting change as a percent-difference from the base-case scenario is reported.

Parameter	**Doubling (x 200%)**	**Halving (x 50%)**
Ambient ^{222}Rn activity in coastal water	-0.01%	+0.01 %
Radon supported by local dissolved ^{226}Ra	-0.1%	+0.01 %
^{222}Rn activity from offshore ^{226}Ra	-0.8%	+0.4%
Residence time of water in the bay	-0.8%	+1.4%
Time series plume thickness	+16.6%	-6.1%
Time series plume area	+100.0%	-50.0%
SGD end-member ^{222}Rn activity	-50.0%	+100.0%

The sensitivity test also showed the horizontal area of the plume has a significant effect on final SGD rates. Considering this issue is shared by nearly all previous studies using this method (e.g. Dulaiova et al., 2010; Swarzenski et al., 2013), we acknowledge that the uncertainty in simplification of the plume geometry is very difficult to constrain and represents a weakness of the method. For this study, since the plume definition was dependent on the survey track, we believe that the plumes were well defined vertically and along the shoreline but are more uncertain in the offshore direction. We also assumed that the geometry of the plumes did not significantly change during the survey period. These limitations should be kept in mind when interpreting the study results.

The SWAT model uses a simplified linear reservoir model for representation of the groundwater system, which applies a single parameter for total groundwater recharge partitioning to the deep aquifer (interpreted here as SGD). Hence, SWAT's SGD results are sensitive to this parameter (Table A3, supplementary material). Additionally, this interpretation hinges on the assumption that watershed boundaries also represent aquifer divides, which is reasonable based on the horizontal bedding of the adjacent geologic units, and estimates of water table elevations from Izuka (1999) and Izuka et al. (2007) that show that the water table conforming closely to the land's surface. Also the hydrologic portion of the SWAT model was calibrated with streamflow data from two stations, (black diamonds in Fig. 2) and therefore different parameter values were assigned for the upper watershed above the quarry, and for the lower watershed below. This was justified geologically, considering that the quarry location coincides with the contact between basalts and alluvium. However, in reality, the local geology is probably heterogeneous, particularly within the basalt unit itself. Thus the bi-modal parameterization of the model area is likely to be somewhat of an oversimplification.

6. Conclusions

By combining a terrestrial and coastal hydrologic field investigation with model-based watershed characterization, we were able to reveal impacts of different nutrient sources and hydrologic pathways in a small American Samoan watershed. This methodological framework demonstrates how snapshot scale observations and transient watershed modeling can be integrated to develop a fairly comprehensive understanding of water and nutrient dynamics in steep watersheds on tropical-basaltic islands. In Faga'alu Watershed, during low-flow conditions, field measurements suggest SGD and nearshore basal-lens baseflow contribute nearly all of the terrigenous DIN to the coastline with high level-baseflow contributing very little. Groundwater discharge was also found to be significant in coastal loading of dissolved PO_4^{3-}. Seepage run measurements indicated groundwater discharge to the stream occurs as two geochemically distinct fractions, (1) high-level baseflow and (2) basal-lens baseflow that discharges near the stream estuary. During baseflow conditions, measurements indicated high-level streamflow contributes about two-thirds of the stream's water, but nearshore basal-lens baseflow contributes the majority of the stream's nutrient load. ^{222}Rn-based measurements suggest that while saltwater recirculation does occur in the shallow portion of the nearshore aquifer, that seawater does not spend sufficient time in the subsurface to pick up a ^{222}Rn signature. The geologic structure of the fringing reef could contain deeper recirculated SGD, but we were not able to confirm the existence of such a source. These field results facilitated the development of a conceptual model of groundwater, surface water, and coastal water interaction within steep basaltic-island watersheds. This conceptual model was foundational for developing the watershed model and interpreting its results.

The SWAT model matched field-estimated water fluxes reasonably well, within 2%, 13%, and 0.3% RPD for basal-lens baseflow, high-level baseflow, and SGD, respectively. The N-transport capabilities of SWAT were also tested; however, limitations in the availability and quality of existing nutrient data prevented satisfactory calibration of this portion of the model.

Overall, field and model results suggest SGD is an important water budget component in this, and likely other geologically similar watersheds. Additionally, because our measurements indicated that both SGD and basal-lens baseflow are likely to be important coastal nutrient loading pathways in these systems, both should be considered when developing nutrient sampling and management plans. Although sampling surface runoff, baseflow, and groundwater nutrients from multiple locations throughout a watershed would require a significant deviation from current water quality management practices in American Samoa, if these data can be collected, they would be very useful for improving upon existing watershed models. Continued development of hydrological models in Faga'alu would be a valuable future research activity for further developing these insights into how groundwater, surface water, and coastal water interact and deliver nutrients to fragile coastal ecosystems.

Acknowledgements

Fa'afetai tele lava to all agencies and individuals who made this work a reality. Alex Messina, Greg McCormick, and Trent Biggs of San Diego State University provided foundational data and collaborative support for development of the SWAT model. Tim Bodell, Mia Comeros, and Jewel Tuiasosopo at American Samoa Environmental Protection Agency, Kristine Bucchianeri at the Coral Reef Advisory Group, and Hideyo Hattori at NOAA contributed valuable scientific support. Abe Voight, Mike Cox, Hugh Fuimaono, Randy DeWees, and Katrina Mariner provided essential logistical assistance on Tutuila and enabled the field component of this work. The authors would also like to thank the village of Faga'alu, the Pulenuu of Faga'alu, and Lisa from the Catholic Church at the stream outlet who generously provided access to the study site. We sincerely appreciate the time and thought put into this manuscript by at least four anonymous reviewers, whose suggestions strengthened the manuscript significantly.

HD acknowledges support from WILL HAVE TO GET YOU THE DETAILS OF THE GRANT. This is contributed paper WRRC-CP-2019-XX of the Water Resources Research Center, University of Hawaii at Manoa, Honolulu, Hawaii. SOEST publication # Funding for this project was provided by the USGS Water Resources Research Institute Program (WRRIP) and NOAA's Pacific Regional Integrated Sciences and Assessments Program (PacRISA) [grant number NA15OAR4310146].

References

Abaya, L.M., Wiegner, T.N., Beets, J.P., Colbert, S.L., Kaile'a, M.C. and Kramer, K.L., 2018a. Spatial distribution of sewage pollution on a Hawaiian coral reef. Marine pollution bulletin, 130, 335-347. https://doi.org/10.1016/j.marpolbul.2018.03.028

Abaya, L.M., Wiegner, T.N., Colbert, S.L., Beets, J.P., Kaile'a, M.C., Kramer, K.L., Most, R. and Couch, C.S., 2018b. A multi-indicator approach for identifying shoreline sewage pollution hotspots adjacent to coral reefs. Marine pollution bulletin, 129(1), 70-80. https://doi.org/10.1016/j.marpolbul.2018.02.005

Abbaspour, K.C., Yang, J., Maximov, I., Siber, R., Bogner, K., Mieleitner, J., Zobrist, J. and Srinivasan, R., 2007. Modelling hydrology and water quality in the pre-alpine/alpine Thur watershed using SWAT. Journal of hydrology, 333(2-4), 413-430. https://doi.org/10.1016/j.jhydrol.2006.09.014

Abbaspour, K.C., 2014. SWAT-CUP 2012: SWAT Calibration and Uncertainty Programs - A User Manual. Sci. Technol. https://swat.tamu.edu/media/114860/usermanual_swatcup.pdf (accessed 2019-03-13).

Abbaspour, K. C., Rouholahnejad, E., Vaghefi, S., Srinivasan, R., Yang, H., & Kløve, B. 2015. A continental-scale hydrology and water quality model for Europe: Calibration and uncertainty of a high-resolution large-scale SWAT model. Journal of Hydrology, 524, 733-752. https://doi.org/10.1016/j.jhydrol.2015.03.027

Amato, D.W., Bishop, J.M., Glenn, C.R., Dulai, H., Smith, C.M., 2016. Impact of submarine groundwater discharge on marine water quality and reef biota of Maui. PLoS One 11, e0165825. https://doi.org/10.1371/journal.pone.0165825

Anderson, M.P., 1987. Field studies in groundwater hydrology—A new era. Reviews of Geophysics, 25(2), 141-147. https://doi.org/10.1029/RG025i002p00141

Armstrong, F.A.J., Stearns, C.R., Strickland, J.D.H., 1967. The measurement of upwelling and subsequent biological process by means of the Technicon Autoanalyzer® and associated equipment, in: Deep-Sea Research and Oceanographic Abstracts. 381–389. https://doi.org/10.1016/0011-7471(67)90082-4

Arnold, J.G., Srinivasan, R., Muttiah, R.S., Williams, J.R., 1998. Large area hydrologic modeling and assessment part I: Model development. J. Am. Water Resour. Assoc. 34, 73–89. https://doi.org/10.1111/j.1752-1688.1998.tb05961.x

ASCC – American Samoa Community College, 2018. Malaeimi weather station data. [Dataset]. https://www.wunderground.com/personal-weather-station/dashboard?ID=IWESTERN499 (accessed 2018-04-30).

AS-EPA - American Samoa Environmental Protection Agency, 2013a. American Samoa Water Quality Standards 2013 Revision Administrative Rule No . 001-2013. https://www.epa.gov/sites/production/files/2014-12/documents/aswqs.pdf (accessed 2019-03-13).

AS-EPA - American Samoa Environmental Protection Agency, 2013b. American Samoa Watershed Management and Protection Program FY12 Annual Report. https://www.epa.as.gov/sites/default/files/documents/surface/FY17%20Watershed%20Report%202018%2005%2021.pdf (accessed 2019-03-13).

AS-EPA - American Samoa Environmental Protection Agency, 2016. Territory of American Samoa Integrated Water Quality Monitoring and Assessment 2016. https://www.epa.as.gov/sites/default/files/documents/public_notice/2016%20AS%20Integrated%20Report%20for%20Public%20Notice%202016%200410%20FINAL.pdf (accessed 2019-03-13).

Avery, E., Bibby, R., Visser, A., Esser, B., Moran, J., 2018. Quantification of groundwater discharge in a subalpine stream using radon-222. Water (Switzerland) 10, 100. https://doi.org/10.3390/w10020100

Bahr, K.D., Jokiel, P.L., Toonen, R.J., 2015. The unnatural history of Kāne‘ohe Bay: coral reef resilience in the face of centuries of anthropogenic impacts. PeerJ 3, e950. https://doi.org/10.7717/peerj.950

Biondi, D., Freni, G., Iacobellis, V., Mascaro, G. and Montanari, A., 2012. Validation of hydrological models: Conceptual basis, methodological approaches and a proposal for a code of practice. Physics and Chemistry of the Earth, Parts A/B/C, 42, 70-76. https://doi.org/10.1016/j.pce.2011.07.037

Bishop, J.M., Glenn, C.R., Amato, D.W. and Dulai, H., 2017. Effect of land use and groundwater flow path on submarine groundwater discharge nutrient flux. Journal of Hydrology: Regional Studies, 11, 194-218. https://doi.org/10.1016/j.ejrh.2015.10.008

Böhlke, J.-K., 2003. Sources, transport, and reaction of nitrate., Residence times and nitrate transport in ground water discharging to streams in the Chesapeake Bay Watershed. Water-Resources Investigations.

Burnett, W.C., Dulaiova, H., 2003. Estimating the dynamics of groundwater input into the coastal zone via continuous radon-222 measurements. J. Environ. Radioact. 69, 21–35. https://doi.org/10.1016/S0265-931X(03)00084-5

Burnett, W.C., Santos, I.R., Weinstein, Y., Swarzenski, P.W. and Herut, B., 2007. Remaining uncertainties in the use of Rn-222 as a quantitative tracer of submarine groundwater discharge. IAHS publication, 312, p.109.

Cartwright, I., Hofmann, H., Sirianos, M.A., Weaver, T.R. and Simmons, C.T., 2011. Geochemical and 222Rn constraints on baseflow to the Murray River, Australia, and timescales for the decay of low-salinity groundwater lenses. Journal of hydrology, 405(3-4), 333-343. https://doi.org/10.1016/j.jhydrol.2011.05.030

Charette, M. a, Moore, W.S., Burnett, W.C., 2007. CHAPTER-5 Uranium-and Thorium-Series Nuclides as Tracers of Submarine Groundwater Discharge CHAPTER-5 Uranium-and Thorium-Series Nuclides as Tracers of Submarine Groundwater Discharge. Uranium 13, 234–289. https://doi.org/10.1016/S1569-4860(07)00005-8

Cole, M.L., Kroeger, K.D., McClelland, J.W., Valiela, I., 2006. Effects of Watershed Land use on Nitrogen Concentrations and delta15 Nitrogen in Groundwater [electronic resource]. Biogeochemistry 77, 199–215. https://doi.org/10.1007/s10533-005-1036-2

Cook, P.G., Wood, C., White, T., Simmons, C.T., Fass, T. and Brunner, P., 2008. Groundwater inflow to a shallow, poorly-mixed wetland estimated from a mass balance of radon. Journal of Hydrology, 354(1-4), 213-226. https://doi.org/10.1016/j.jhydrol.2008.03.016

Corbett, D.R., Chanton, J., Burnett, W., Dillon, K., Rutkowski, C. and Fourqurean, J.W., 1999. Patterns of groundwater discharge into Florida Bay. Limnology and Oceanography, 44(4), 1045-1055. https://doi.org/10.4319/lo.1999.44.4.1045

Craig, P., 2009. Natural history guide to American Samoa, 3rd edition. Department of Marine and Wildlife Resources, Pago Pago. https://lccn.loc.gov/2007390401

Dadhich, A. P., & Nadaoka, K., 2012. Analysis of terrestrial discharge from agricultural watersheds and its impact on nearshore and offshore reefs in Fiji. Journal of Coastal Research, 28(5), 1225-1235. https://doi.org/10.2112/JCOASTRES-D-11-00149.1

Dailer, M.L., Knox, R.S., Smith, J.E., Napier, M. and Smith, C.M., 2010. Using $\delta^{15}N$ values in algal tissue to map locations and potential sources of anthropogenic nutrient inputs on the island of Maui, Hawaiʻi, USA. Marine Pollution Bulletin, 60(5), 655-671. https://doi.org/10.1016/j.marpolbul.2009.12.021

Davis, D., 1963. Groundwater reconnaissance of American Samoa. U.S. Geological Survey Report No. 1608-C. US Government Printing Office.

DiDonato, G. T., 2004. ASEPA Stream Monitoring: Results from Year 1 and Preliminary Interpretation. Report for the American Samoa Environmental Protection Agency. http://www.botany.hawaii.edu/basch/uhnpscesu/pdfs/sam/DiDonato2004ASEPAAS.pdf (accessed 2019-06-24)

DiDonato, G.T., 2005. Nitrogen and phosphorus concentrations in tropical Pacific insular streams: historical data from Tutuila, American Samoa. Micronesica-Agana- 37, 235.

Downer, C.W., Ogden, F.L., 2006. Gridded Surface Subsurface Hydrologic Analysis (GSSHA) User's Manual, Version 1.43 for Watershed Modeling System 6.1, US Army Corps of Engineers, Engineer Research and Development Center. https://doi.org/10.21236/ADA455335

Dulai, H., Kleven, A., Ruttenberg, K., Briggs, R. and Thomas, F., 2016. Evaluation of submarine groundwater discharge as a coastal nutrient source and its role in coastal groundwater quality and quantity. In Emerging Issues in Groundwater Resources 187-22. https://doi.org/10.1007/978-3-319-32008-3_8

Dulaiova, H., Burnett, W.C., Wattayakorn, G., Sojisuporn, P., 2006. Are groundwater inputs into river-dominated areas important? The Chao Phraya River - Gulf of Thailand. Limnol. Oceanogr. 51, 2232–2247. https://doi.org/10.4319/lo.2006.51.5.2232

Dulaiova, H., Camilli, R., Henderson, P.B., Charette, M.A., 2010. Coupled radon, methane and nitrate sensors for large-scale assessment of groundwater discharge and non-point source pollution to coastal waters. J. Environ. Radioact. 101, 553–563. https://doi.org/10.1016/j.jenvrad.2009.12.004

Falkland, T., Carpenter, C., Stubbs, J., Overmars, M., 2002. Proceedings of the Pacific Regional Consultation on Water in Small Island Countries. Pacific Community (SPC) http://www.pacificwater.org/userfiles/file/Water%20in%20Small%20Island%20Country%20proceeding.pdf (accessed 2015-09-24)

Fenech, C., Rock, L., Nolan, K., Tobin, J. and Morrissey, A., 2012. The potential for a suite of isotope and chemical markers to differentiate sources of nitrate contamination: a review. Water Research, 46(7), 2023-2041. https://doi.org/10.1016/j.watres.2012.01.044

Fröllje, H., Fitzsimmons, J.N., Dulai, H., Schnetger, B., Brumsack, H.-J., Pahnke, K., 2016. Hawaiian imprint on dissolved Nd and Ra isotopes and rare earth elements in the central North Pacific: Local survey and seasonal variability. Geochim. Cosmochim. Acta 189, 110–131. https://doi.org/10.1016/j.gca.2016.06.001

Gassman, P. W., Reyes, M. R., Green, C. H., Arnold, J. G., 2007. The Soil and Water Assessment Tool: Historical Development, Applications, and Future Research Directions. Trans. ASABE 50, 1211–1250. https://doi.org/10.13031/2013.23637

Gassman, P.W., Sadeghi, A.M., Srinivasan, R., 2014. Applications of the SWAT Model Special Section: Overview and Insights. J. Environ. Qual. 43, 1. https://doi.org/10.2134/jeq2013.11.0466

Garrison, G. H., Glenn, C. R., & McMurtry, G. M. 2003. Measurement of submarine groundwater discharge in Kahana Bay, O'ahu, Hawai'i. Limnology and Oceanography, 48(2), 920-928. https://doi.org/10.4319/lo.2003.48.2.0920

Garrison, V., Kroeger, K., Fenner, D., Craig, P., 2007. Identifying nutrient sources to three lagoons at Ofu and Olosega, American Samoa using δ15N of benthic macroalgae. Mar. Pollut. Bull. 54, 1830–1838. https://doi.org/10.1016/j.marpolbul.2007.08.016

Genereux, D.P., Hemond, H.F. and Mulholland, P.J., 1993. Use of radon-222 and calcium as tracers in a three-end-member mixing model for streamflow generation on the West Fork of Walker Branch Watershed. Journal of Hydrology, 142(1-4), 167-211. https://doi.org/10.1016/0022-1694(93)90010-7

Gleeson, J., Santos, I.R., Maher, D.T., Golsby-Smith, L., 2013. Groundwater-surface water exchange in a mangrove tidal creek: Evidence from natural geochemical tracers and implications for nutrient budgets. Mar. Chem. 156, 27–37. https://doi.org/10.1016/j.marchem.2013.02.001

Gleeson, T., Manning, A.H., Popp, A., Zane, M., Clark, J.F., 2018. The suitability of using dissolved gases to determine groundwater discharge to high gradient streams. J. Hydrol. 557, 561–572. https://doi.org/10.1016/j.jhydrol.2017.12.022

Glenn, C.R., Whittier, R.B., Dailer, M.L., Dulaiova, H., El-kadi, A.I., Fackrell, J., Sevadjian, J., 2013. Lahaina Groundwater Tracer Study —Lahaina, Maui, Hawaii. Final Interim Report prepared from the State of Hawaii DOH, the U.S. EPA, and the U.S. Army Engineer Research and Development Center https://scholarspace.manoa.hawaii.edu/handle/10125/50768 (accessed 2019-03-13).

Grasshoff, K., Ehrhardt, M., Kremling, K., 1999. Methods of Seawater Analysis. Second, Revised and Extended Edition, 3rd ed. John Wiley & Sons. https://doi.org/10.1002/9783527613984

Guo W, Langevin CD. 2002. User’s guide to SEAWAT: a computer program for simulation of three-dimensional variable-density groundwater flow. US Geological Survey, Techniques of Water-Resources Investigations 6-A7.

Guzman, J.A., Moriasi, D.N., Gowda, P.H., Steiner, J.L., Starks, P.J., Arnold, J.G., Srinivasan, R., 2015. Environmental Modelling & Software A model integration framework for linking SWAT and MODFLOW. Environ. Model. Softw. 73, 103–116. https://doi.org/10.1016/j.envsoft.2015.08.011

Houben, G.J., Stoeckl, L., Mariner, K.E. and Choudhury, A.S., 2018. The influence of heterogeneity on coastal groundwater flow-physical and numerical modeling of fringing reefs, dykes and structured conductivity fields. Advances in water resources, 113, 155-166. https://doi.org/10.1016/j.advwatres.2017.11.024

Houk, P., Didonato, G., Iguel, J., & Van Woesik, R., 2005. Assessing the effects of non-point source pollution on American Samoa’s coral reef communities. Environ. Monit. Assess. 107, 11–27. https://doi.org/10.1007/s10661-005-2019-4

Houk, P., Benavente, D., Johnson, S., 2013. Watershed-based coral reef monitoring across Tutuila, American Samoa - Summary of decadal trends and 2013 assessment.

Hunt, C.D., 2007. Ground-Water Nutrient Flux to Coastal Waters and Numerical Simulation of Wastewater Injection at Kihei , Maui , Hawaii. USGS Open Report 2006, 5283. https://pubs.usgs.gov/sir/2006/5283/sir2006-5283.pdf (accessed 2019-03-13).

Hunt, Charles D., J., Rosa, S.N., 2009. A Multitracer Approach to Detecting Wastewater Plumes from Municipal Injection Wells in Nearshore Marine Waters at Kihei and Lahaina, Maui, Hawaii (USGS Scientific Investigations Report 2009-5253) 166.

Izuka, S.K., 1999, Hydrogeologic interpretations from available ground-water data, Tutuila, American Samoa: U.S. Geological Survey Water-Resources Investigations Report 99-4064, 2 sheets.

Izuka, S.K., Perreault, J.A., Presley, T.K., 2007. Areas contributing recharge to wells in the Tafuna-Leone Plain, Tutuila, American Samoa: U.S. Geological Survey Scientific Investigations Report 2007-5167. https://pubs.usgs.gov/sir/2007/5167/ (accessed 2019-07-13).

Jacob, N., Babu, D.S. and Shivanna, K., 2009. Radon as an indicator of submarine groundwater discharge in coastal regions. Current Science, 1313-1320.

Jarsjö, J., Destouni, G., Persson, K. and Prieto, C., 2007. Solute transport in coupled inland-coastal water systems. General conceptualisation and application to Forsmark (No. SKB-R--07-65). Swedish Nuclear Fuel and Waste Management Co.

Johannes, R.E., Hearn, C.J., 1985. The effect of submarine groundwater discharge on nutrient and salinity regimes in a coastal lagoon off Perth, Western Australia. Estuar. Coast. Shelf Sci. 21, 789–800. https://doi.org/10.1016/0272-7714(85)90073-3

Kampf, S.K., Burges, S.J., 2007. A framework for classifying and comparing distributed hillslope and catchment hydrologic models. Water Resour. Res. 43. https://doi.org/10.1029/2006WR005370

Kelly, J.L., Glenn, C., 2012. Identification and quantification of submarine groundwater discharge in the Hawaiian Islands. Doctoral dissertation Dept. of . Geology and Geophysics, University of Hawaii at Manoa.

Kendall, C., 2012. Tracing Nitrogen Sources and Cycling in Catchments, in: Isotope Tracers in Catchment Hydrology. Elsevier, 519–576. https://doi.org/10.1016/b978-0-444-81546-0.50023-9

Kendall, C., Aravena, R., 2000. Nitrate Isotopes in Groundwater Systems, in: Environmental Tracers in Subsurface Hydrology. Springer, 261–297. https://doi.org/10.1007/978-1-4615-4557-6_9

Kimsey, M. B., 2005. Implementation guidance for the ground water quality standards. Washington State Department of Ecology Publication, (96-02). https://fortress.wa.gov/ecy/publications/documents/9602.pdf (accessed 2019-06-20)

Kirchner, J.W., 2006. Getting the right answers for the right reasons: Linking measurements, analyses, and models to advance the science of hydrology. Water Resources Research, 42(3). https://doi.org/10.1029/2005WR004362

Kim, N. W., Chung, I. M., Won, Y. S., & Arnold, J.G., 2008. Development and application of the integrated SWAT-MODFLOW model. Journal. of. Hydrol. 356, 1–16. https://doi.org/10.1016/j.jhydrol.2008.02.024

Kirs, M., Harwood, V.J., Fidler, A.E., Gillespie, P.A., Fyfe, W.R., Blackwood, A.D. and Cornelisen, C.D., 2011. Source tracking faecal contamination in an urbanised and a rural waterway in the Nelson-Tasman region, New Zealand. New Zealand Journal of Marine and Freshwater Research, 45(1), pp.43-58. https://doi.org/10.1080/00288330.2010.535494

Knee, K. L., Crook, E. D., Hench, J. L., Leichter, J. J., & Paytan, A., 2016. Assessment of submarine groundwater discharge (SGD) as a source of dissolved radium and nutrients to Moorea (French Polynesia) coastal waters. Estuaries and coasts, 39(6), 1651-1668. https://doi.org/10.1007/s12237-016-0108-y

Krall, A.L., Elliott, S.M., Erickson, M.L., Adams, B.A., 2018. Detecting sulfamethoxazole and carbamazepine in groundwater: Is ELISA a reliable screening tool? Environ. Pollut. 234, 420–428. https://doi.org/10.1016/j.envpol.2017.11.065

Kuan, W.K., G. Jin, P. Xin, C. Robinson, B. Gibbes, and L. Li., 2012. Tidal influence on seawater intrusion in unconfined coastal aquifers. Water Resources Research 48: W02502. https://doi.org/10.1029/2011WR010678

Lee, J.M. and Kim, G., 2007. Estimating submarine discharge of fresh groundwater from a volcanic island using a freshwater budget of the coastal water column. Geophysical Research Letters, 34(11). https://doi.org/10.1029/2007GL029818

Lindau, Delaune, Patr, 1989. Assessment of stable n isotopes in fingerprinting surface water n source. Water. Air. Soil Pollut. 48, 489–496. https://doi.org/10.1007/BF00283346

Makings, U., Santos, I.R., Maher, D.T., Golsby-Smith, L., Eyre, B.D., 2014. Importance of budgets for estimating the input of groundwater-derived nutrients to an eutrophic tidal river and estuary. Estuar. Coast. Shelf Sci. 143, 65–76. https://doi.org/10.1016/j.ecss.2014.02.003

McCook, L.J., 1999. Macroalgae, nutrients and phase shifts on coral reefs: Scientific issues and management consequences for the Great Barrier Reef. Coral Reefs 18, 357–367. doi:10.1007/s003380050213

McCormick, G.R., 2017. Water Quality and Sources of Nutrient Loads in Watersheds of American Samoa. Masters thesis, Dept. of Geography, San Diego State University. https://search.proquest.com/openview/a236c90fb2b272eab29080873da04169/1?pq-origsite=gscholar&cbl=18750&diss=y (accessed 2019-03-13).

Messina, A.T., 2016. Terrigenous Sediment Dynamics in a Small, Tropical Fringing-Reef Embayment, American Samoa. Doctoral dissertation Dept. of Geography, University of California, Santa Barbara. https://www.alexandria.ucsb.edu/lib/ark:/48907/f3sj1kpt (accessed 2019-03-13).

Messina, A.M., Biggs, T.W., 2016. Contributions of human activities to suspended sediment yield during storm events from a small, steep, tropical watershed. J. Hydrol. 538, 726–742. https://doi.org/10.1016/j.jhydrol.2016.03.053

Michael, H.A., 2005. Seasonal dynamics in costal aquifers: investigation of submarine groundwater discharge through field measurements and numerical models (Doctoral dissertation, Massachusetts Institute of Technology).

Moosdorf, N., Stieglitz, T., Waska, H., Dürr, H., Hartmann, J., 2015. Submarine groundwater discharge from tropical islands: a review. Grundwasser 20, 53–67. https://doi.org/10.1007/s00767-014-0275-3

Nakada, S., Yasumoto, J., Taniguchi, M. and Ishitobi, T., 2011. Submarine groundwater discharge and seawater circulation in a subterranean estuary beneath a tidal flat. Hydrological Processes, 25(17), 2755-2763. https://doi.org/10.1002/hyp.8016

Nakamura, S., 1984. Soil Survey of American Samoa. USDA Soil Conservation Service, Washington, DC. 95 pp

Nash, J.E. and Sutcliffe, J.V., 1970. River flow forecasting through conceptual models part I—A discussion of principles. Journal of hydrology, 10(3), 282-290.

NGDC, 2013. American Samoa 1/3 Arc-second MWH Coastal Digital Elevation Model [dataset]. https://catalog.data.gov/dataset/pago-pago-american-samoa-coastal-digital-elevation-model34341 (accessed 2015-12-10).

N.J.A.C. - New Jersey Administrative Code., 2018. Ground Water Quality Standards https://www.nj.gov/dep/rules/rules/njac7_9c.pdf (accessed 2019-06-20)

NRC - National Research Council, 2004. Assessing the national streamflow information program. National Academies Press.

Oberdorfer, J.A., 2003. Hydrogeologic modeling of submarine groundwater discharge: Comparison to other quantitative methods. Biogeochemistry 66, 159–169. https://doi.org/10.1023/B:BIOG.0000006096.94630.54

Oki, D.S., Souza, W.R., Bolke, E.L., Bauer, G.R., 1998. Numerical analysis of the hydrogeologic controls in a layered coastal aquifer system, Oahu, Hawaii, USA. Hydrogeol. J. 6, 243–263. https://doi.org/10.1007/s100400050149

Peterson, R. N., Burnett, W. C., Taniguchi, M., Chen, J., Santos, I. R., & Ishitobi, T., 2008. Radon and radium isotope assessment of submarine groundwater discharge in the Yellow River delta, China. Journal of Geophysical Research: Oceans, 113(C9). https://doi.org/10.1029/2008JC004776

Peterson, R.N., Santos, I.R., Burnett, W.C., 2010. Evaluating groundwater discharge to tidal rivers based on a Rn-222 time-series approach. Estuar. Coast. Shelf Sci. 86, 165–178. https://doi.org/10.1016/j.ecss.2009.10.022

Petrie, B., Barden, R. and Kasprzyk-Hordern, B., 2015. A review on emerging contaminants in wastewaters and the environment: current knowledge, understudied areas and recommendations for future monitoring. Water research, 72, pp.3-27. https://doi.org/10.1016/j.watres.2014.08.053

Polidoro, B.A., Comeros-Raynal, M.T., Cahill, T., Clement, C., 2017. Land-based sources of marine pollution: Pesticides, PAHs and phthalates in coastal stream water, and heavy metals in coastal stream sediments in American Samoa. Mar. Pollut. Bull. 116, 501–507. https://doi.org/10.1016/j.marpolbul.2016.12.058

Robinson, C., L. Li, and D.A. Barry., 2007. Effect of tidal forcing on a subterranean estuary. Advances in Water Resources 30: 851–865. https://doi.org/10.1016/j.advwatres.2006.07.006

Rodellas, V., Garcia-Orellana, J., Masqué, P., Feldman, M. and Weinstein, Y., 2015. Submarine groundwater discharge as a major source of nutrients to the Mediterranean Sea. Proceedings of the National Academy of Sciences, 112(13), 3926-3930. https://doi.org/10.1073/pnas.1419049112

Rogers, K.M., Nicolini, E., Gauthier, V., 2012. Identifying source and formation altitudes of nitrates in drinking water from Réunion Island, France, using a multi-isotopic approach. J. Contam. Hydrol. 138–139, 93–103. https://doi.org/10.1016/j.jconhyd.2012.07.002

Rosenberry, D.O., LaBaugh, J.W., 2008. Field Techniques for Estimating Water Fluxes Between Surface Water and Ground Water Techniques and Methods 4 – D2, U. S. Geological Survey. https://doi.org/10.3133/tm4D2

Sadat-Noori, M., Santos, I.R., Sanders, C.J., Sanders, L.M., Maher, D.T., 2015. Groundwater discharge into an estuary using spatially distributed radon time series and radium isotopes. J. Hydrol. 528, 703–719. https://doi.org/10.1016/j.jhydrol.2015.06.056

Sauafea-Le'au, F., 2013. Faga'alu Village watershed management and conservation plan: American Samoa, 2012-2013. Prepared by the Village of Faga’alu, NOAA- Coral Reef Conservation Program. Pago Pago AS. https://repository.library.noaa.gov/view/noaa/727/noaa_727_DS1.pdf (accessed 2019-07-13)

Sauer, V. B., and Meyer, R. W., 1992. Determination of error in individual discharge measurements: U.S. Geological Survey, Open-File Report 92-144, 21p. https://doi.org/10.3133/ofr92144

Schubert, M., Petermann, E., Stollberg, R., Gebel, M., Scholten, J., Knöller, K., ... & Weiß, H., 2019. Improved Approach for the Investigation of Submarine Groundwater Discharge by Means of Radon Mapping and Radon Mass Balancing. Water, 11(4), 749. https://doi.org/10.3390/w11040749

Scott, T.M., Rose, J.B., Jenkins, T.M., Farrah, S.R., 2002. Microbial Source Tracking : Current Methodology and Future Directions †. Appl. Environ. Microbiol. 68, 5796–5803. https://doi.org/10.1128/AEM.68.12.5796

Shuler, C.K., El-Kadi, A.I., Dulai, H., Glenn, C.R., Fackrell, J., 2017. Source partitioning of anthropogenic groundwater nitrogen in a mixed-use landscape, Tutuila, American Samoa. Hydrogeol. J. 25, 2419–2434. https://doi.org/10.1007/s10040-017-1617-x

Sigman, D.M., Casciotti, K.L., Andreani, M., Barford, C., Galanter, M., Bo, J.K., Supe, Ä.N., 2001. A Bacterial Method for the Nitrogen Isotopic Analysis of Nitrate in Seawater and Freshwater 73, 4145–4153. https://doi.org/10.1021/ac010088e

Slack, J. R., & Landwehr, J. M., 1992. Hydro-climatic data network (HCDN); a US Geological Survey streamflow data set for the United States for the study of climate variations, 1874-1988 (No. 92-129). US Geological Survey, https://doi.org/10.3133/ofr92129

Stearns, H.T., 1944. Geology of the Samoan Islands. Geol. Soc. Am. Bull. 55, 1279–1332. https://doi.org/10.1130/gsab-55-1279

Storlazzi, C., Messina, A., Cheriton, O., Biggs, T., 2014. Eulerian and Lagrangian Measurements of Water Flow and Residence Time in a Fringing Coral Reef Embayment, in: AGU Fall Meeting Abstracts.

Storlazzi, C.D., Cheriton, O.M., Messina, A.M. and Biggs, T.W., 2018. Meteorologic, oceanographic, and geomorphic controls on circulation and residence time in a coral reef-lined embayment: Faga'alu Bay, American Samoa. Coral Reefs, 37(2), 457-469. https://doi.org/10.1007/s00338-018-1671-4

Street, J.H., Knee, K.L., Grossman, E.E., Paytan, A., 2008. Submarine groundwater discharge and nutrient addition to the coastal zone and coral reefs of leeward Hawai'i. Mar. Chem. 109, 355–376. doi:10.1016/j.marchem.2007.08.009

Swarzenski, P.W., Dulaiova, H., Dailer, M.L., Glenn, C.R., Smith, C.G. and Storlazzi, C.D., 2013. A geochemical and geophysical assessment of coastal groundwater discharge at select sites in Maui and O'ahu, Hawai'i. In Groundwater in the Coastal Zones of Asia-Pacific (pp. 27-46). Springer, Dordrecht. https://doi.org/10.1007/978-94-007-5648-9_3

Takasaki, K.J., Mink, J.F., 1985. Evaluation of major dike-impounded ground-water reservoirs, Island of Oahu, U.S. Geological Survey Water Supply Paper 2217. US Government Printing Office Washington, DC.

Turnipseed, P., Sauer, V.B., 2010. Discharge measurements at gaging stations. Tec. o Water-Resources Investig. United States Geol. Surv. - B. 3 - Appl. Hydarulics 171. https://doi.org/10.3133/tm3A8

Unland, N.P., Cartwright, I., Rau, G.C., Reed, J., Gilfedder, B.S., Atkinson, A.P. and Hofmann, H., 2013. Investigating the spatio-temporal variability in groundwater and surface water interactions: a multi-technique approach. Hydrology and Earth System Sciences, 17(9), 3437. https://doi.org/10.5194/hess-17-3437-2013

Van Griensven, A. V., Meixner, T., Grunwald, S., Bishop, T., Diluzio, M., & Srinivasan, R., 2006. A global sensitivity analysis tool for the parameters of multi-variable catchment models. Journal of hydrology, 324(1-4), 10-23. https://doi.org/10.1016/j.jhydrol.2005.09.008

Vetter, O., Vargas-Angel, B., 2014. CRCP Project # 417 : Inter-Disciplinary Study of Flow Dynamics and Sedimentation Effects on Coral Colonies in Faga'alu Bay, American Samoa : Oceanographic Investigation Summary. Pago Pago.

Wang, X., Li, H., Yang, J., Zheng, C., Zhang, Y., An, A., Zhang, M. and Xiao, K., 2017. Nutrient inputs through submarine groundwater discharge in an embayment: A radon investigation in Daya Bay, China. Journal of hydrology, 551, 784-792. https://doi.org/10.1016/j.jhydrol.2017.02.036

WASY, 2004. Feflow 5.1 Finite Element Subsurface Flow & Transport Simulation System User's Manual, WASY Institute for Water Resources Planning and Systems Research Ltd., Berlin, Germany. http://feflow.info/fileadmin/FEFLOW/content_feflow61/users_manual.pdf (accessed 2019-07-13)

Whitall, D.R., Holst, S., 2015. Pollution in surface sediments in Faga'alu Bay, Tutuila, American Samoa. NOAA Technical Memorandum NOS NCCOS 201. Silver Spring, MD. 1-54 https://coastalscience.noaa.gov/data_reports/pollution-in-surface-sediments-in-fagaalu-bay-tutuila-american-samoa/ (accessed 2019-03-13).

Wiegner, T.N., Mokiao-Lee, A.U., Johnson, E.E., 2016. Identifying nitrogen sources to thermal tide pools in Kapoho, Hawai'i, U.S.A, using a multi-stable isotope approach. Mar. Pollut. Bull. 103, 63–71. https://doi.org/10.1016/j.marpolbul.2015.12.046

Wong, W.W., Grace, M.R., Cartwright, I., Cook, P.L.M., 2014. Sources and fate of nitrate in a groundwater-fed estuary elucidated using stable isotope ratios of nitrogen and oxygen. Limnol. Oceanogr. 59, 1493–1509. https://doi.org/10.4319/lo.2014.59.5.1493

Xue, D., Botte, J., De Baets, B., Accoe, F., Nestler, A., Taylor, P., Van Cleemput, O., Berglund, M. and Boeckx, P., 2009. Present limitations and future prospects of stable isotope methods for nitrate source identification in surface-and groundwater. Water research, 43(5), 1159-1170. https://doi.org/10.1016/j.watres.2008.12.048

Zektser, I.S., Everett, L.G., 2000. Groundwater and the Environment: Applications for the Global Community. CRC Press. https://doi.org/10.1201/9781420032895

Zhu, A., Saito, M., Onodera, S.I., Shimizu, Y., Jin, G., Ohta, T. and Chen, J., 2019. Evaluation of the spatial distribution of submarine groundwater discharge in a small island scale using the ^{222}Rn tracer method and comparative modeling. Marine Chemistry, 209, 25-35. https://doi.org/10.1016/j.marchem.2018.12.003

Figures

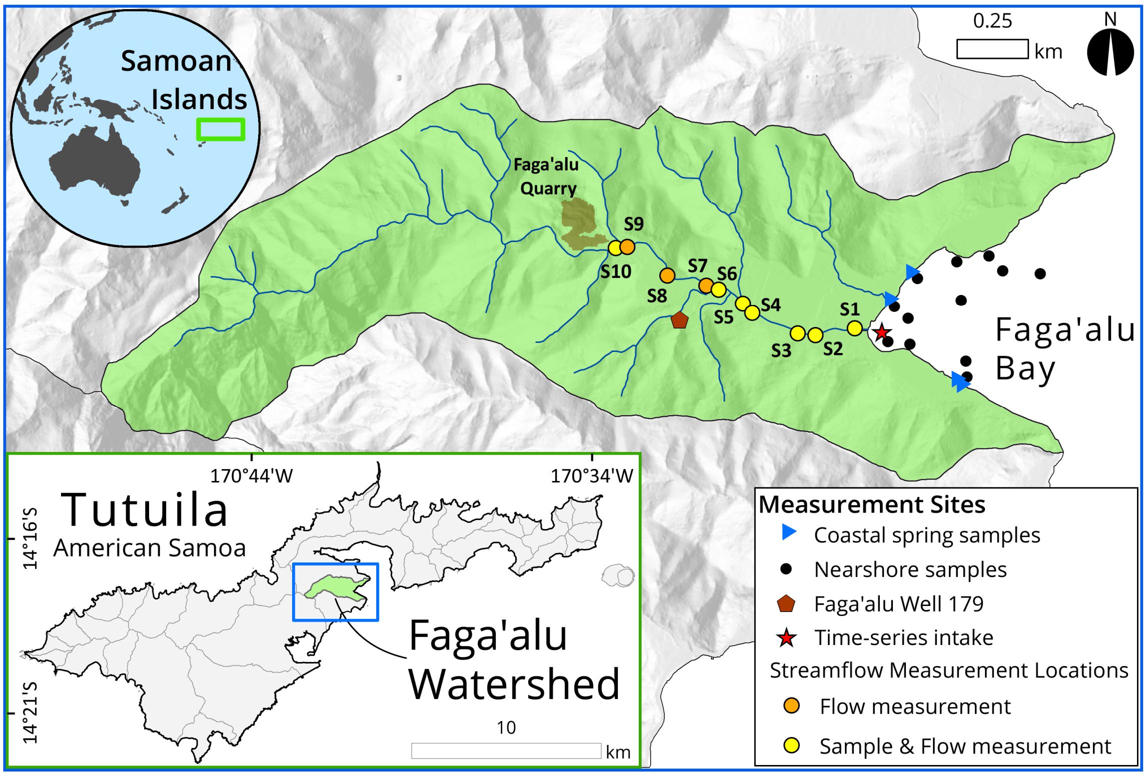

Figure 1: Study area and locations of sample sites in stream (colored circles), well (pentagon), coastal springs (triangles), and nearshore waters (black circles). Flow measurements were taken at all stream sites and yellow circles indicate where water samples were taken as well. The seepage run focused on the lower reach of Faga’alu Stream (below the quarry) as this reach encompassed the majority of human development within the valley.

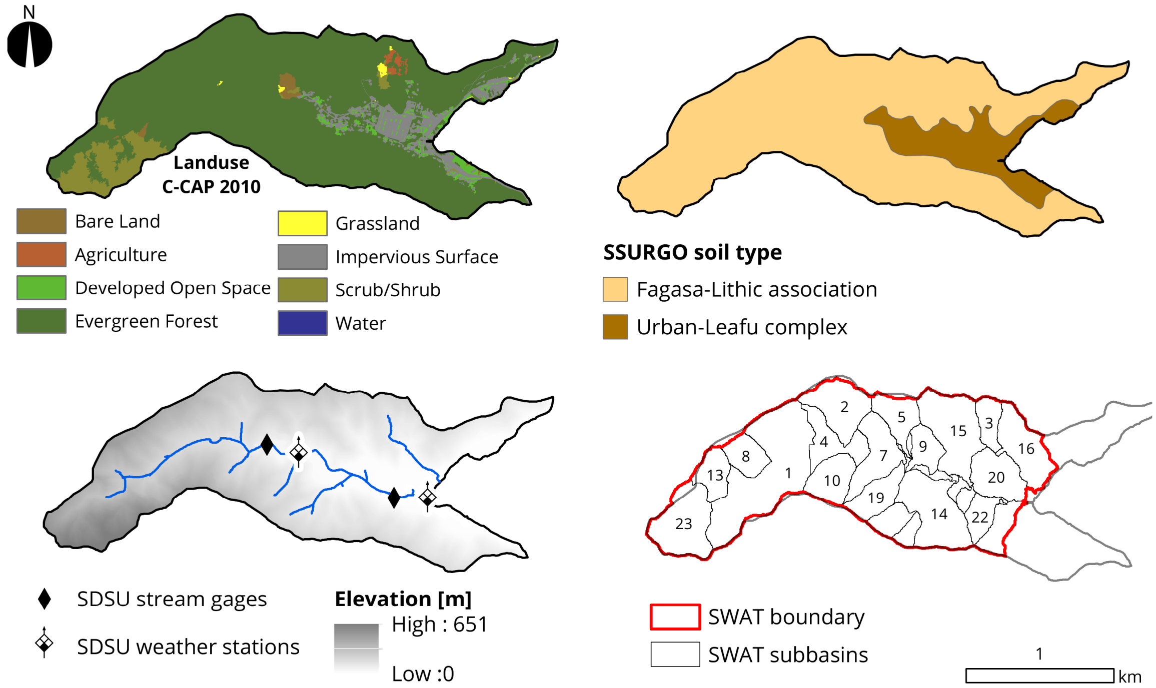

Figure 2: Input datasets used in SWAT model. These included (clockwise from top left) 1) land-use type, 2) soil type, 3) model boundaries, and 4) land surface elevation, and locations of weather and streamflow monitoring points.

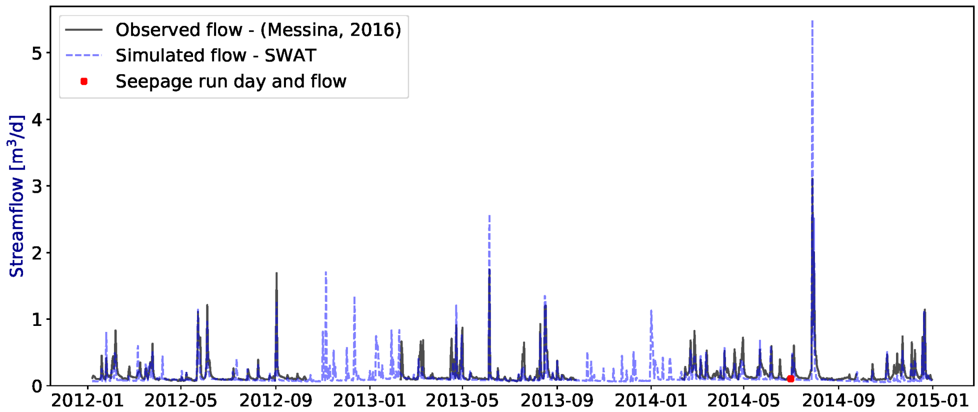

Figure 3: Daily streamflow hydrograph showing observed flow (from Messina, 2016) (black line) and SWAT modeled flow (blue dashed line). The date and flow value of our seepage run is indicated for comparative purposes (red dot).

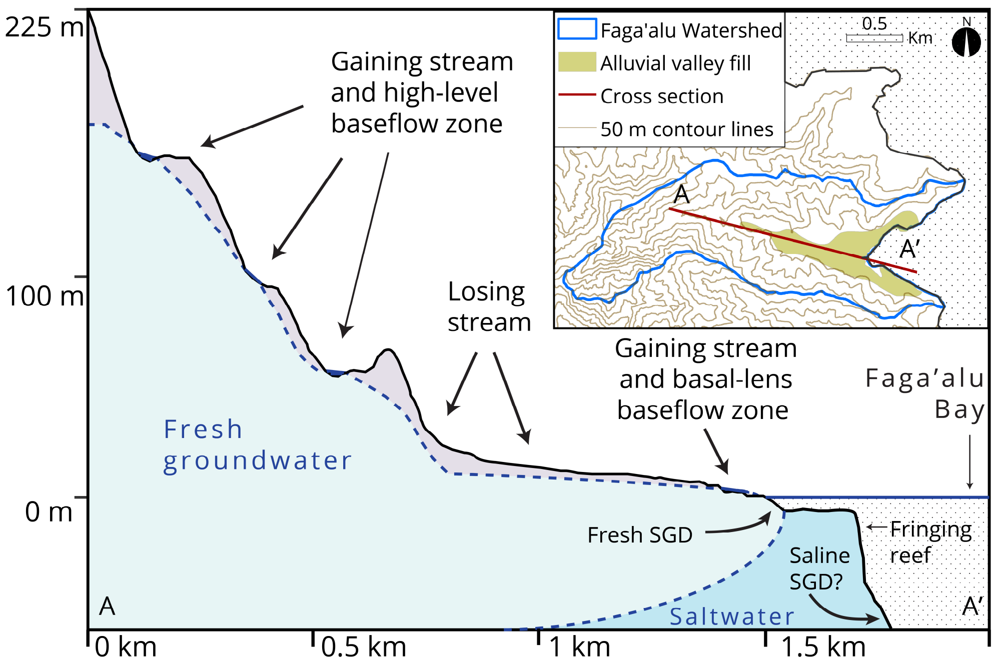

Figure 4: Conceptual schematic cross-section of groundwater-surface water interaction during baseflow conditions in Faga'alu watershed, based on geological information, geochemical data, and physical observations. The stream gains from high-level groundwater in its upper section and upon reaching the more permeable alluvial fill on the valley floor, begins to slowly lose water. The stream again intersects the water table near the coast where basal-lens groundwater discharges to the nearshore stream reach. Upper right panel shows map view of the valley topography and extent of alluvial valley fill.

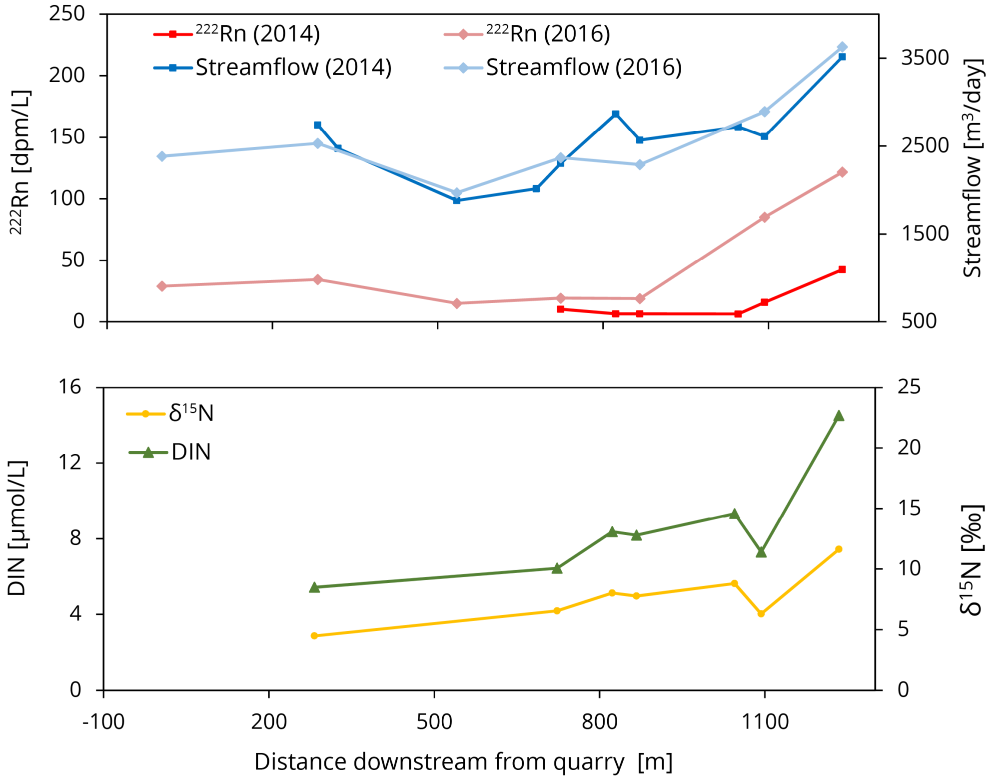

Figure 5: Physical (streamflow) and geochemical (^{222}Rn, DIN, and δ^{15}N) measurements from sampling points along seepage runs. The stream mouth, where the stream discharges into the bay, is located 1,250 m downstream from Faga'alu quarry, which marks the upper boundary of the lower reach of Faga'alu stream. Streamflow measurement uncertainty was not directly assessed, but was assumed to be 10% of the measurement value, and analytical uncertainties are within symbol sizes. Note that for validation purposes, the same seepage run was reproduced in August 2016. Streamflow and ^{222}Rn data from both 2014 and 2016 seepage runs are shown in top graph. The 2016 data is shown for validation only; all calculations were performed with 2014 data.

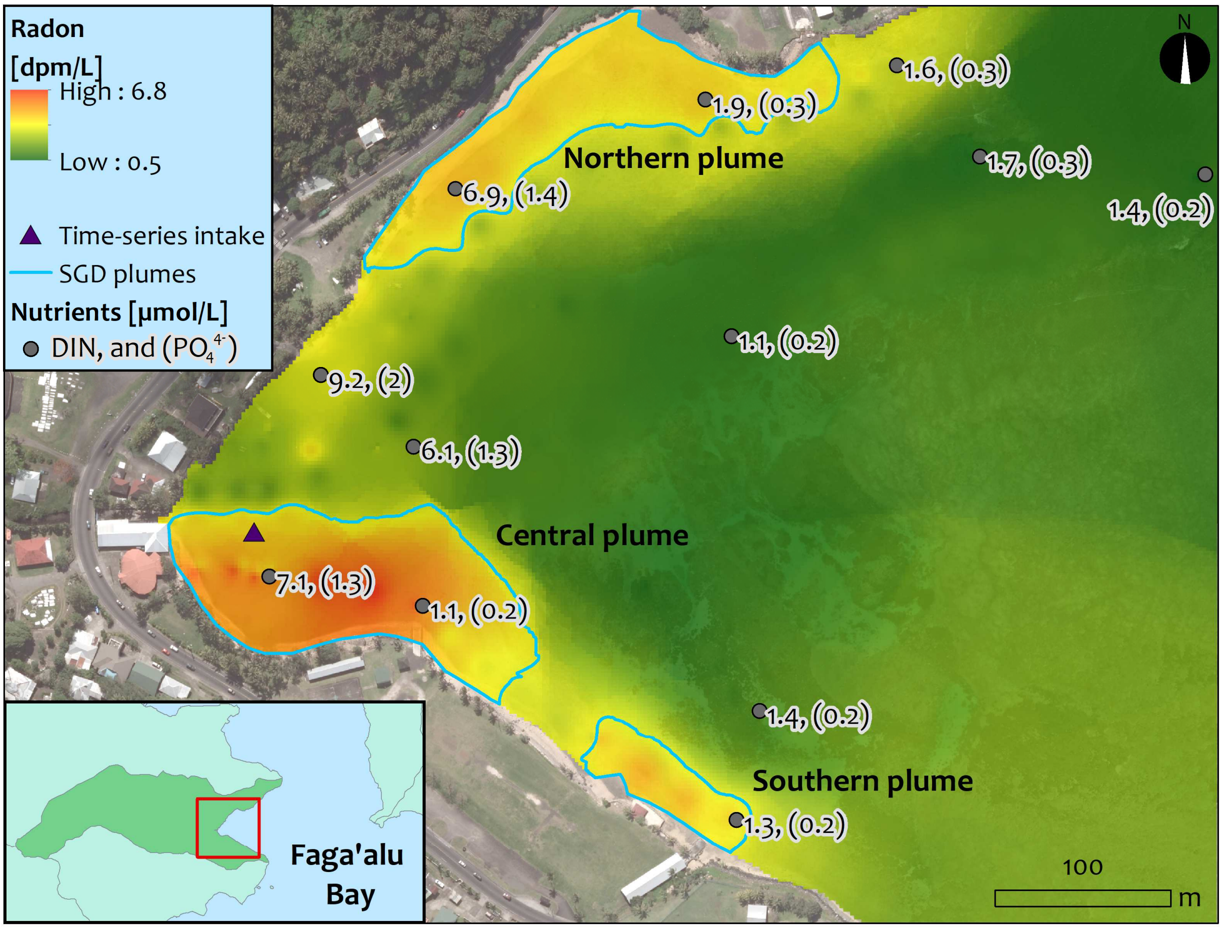

Figure 6: Results from coastal radon survey and surface water nutrient sampling. Dissolved radon concentrations are higher near the coast, indicating areas of groundwater discharge. Blue lines indicate defined boundaries of groundwater plumes, based on ^{222}Rn iso-lines of 3.5 dpm/L. Water sample locations (grey dots) and concentrations of DIN (first number) and PO_4^{3-} (second number inside parentheses) are also shown in µmol/L.